Onecut factors and Pou2f2 regulate diversification and migration of V2 interneurons in the mouse developing spinal cord

Audrey Harris[1], Gauhar Masgutova[1], Amandine Collin[1], Mathilde Toch[1], Maria Hidalgo-Figueroa[1,4], Benvenuto Jacob[2], Lynn M. Corcoran[3], Cédric Francius[1,5] and Frédéric Clotman[1*]

[1] Université catholique de Louvain, Institute of Neuroscience, Laboratory of Neural Differentiation, Brussels, Belgium; [2] Université catholique de Louvain, Institute of Neuroscience, System and Cognition division, Brussels, Belgium; [3] The Walter and Eliza Hall Institute, Molecular Immunology Division and Immunology Division, Parkville, Victoria, Australia.

For correspondence : frederic.clotman@uclouvain.be

[4] Present address : Neuropsychopharmacology & Psychobiology Research Group, Area of Psychobiology, Department of Psychology, University of Cadiz, Spain; Instituto de Investigación e Innovación en Ciencias Biomédicas de Cádiz (INiBICA), Spain

[5] Present address : PAREXEL International, France

Abstract

Acquisition of proper neuronal identity and position is critical for the formation of neural circuits. In the embryonic spinal cord, cardinal populations of interneurons diversify into specialized subsets and migrate to defined locations within the spinal parenchyma. However, the factors that control interneuron diversification and migration remain poorly characterized. Here, we show that the Onecut transcription factors are necessary for proper diversification and migration of the spinal V2 interneurons in the developing spinal cord. Furthermore, we uncover that these proteins restrict and moderate the expression of spinal isoforms of *Pou2f2*, a transcription factor known to regulate B-cell differentiation. By gain- or loss-of-function experiments, we show that Pou2f2 contribute to regulate the distribution of V2 populations in the developing spinal cord. Thus, we uncovered a genetic pathway that regulates the diversification and the migration of V2 interneurons during embryonic development.

Introduction

Neuronal migration is a critical feature of CNS development. It enables neurons, which initiate differentiation in the vicinity of the ventricular zone wherein neural progenitors are located, to reach adequate location in the nervous parenchyma and properly integrate into neural circuits. The mechanisms that regulate neuronal migration have been extensively studied in the developing brain, particularly for cortical interneurons (INs) that are produced in the ganglionic eminences and undergo a long tangential displacement to invade the cortex and integrate into cortical circuits (Barber and Pierani 2016, Guo and Anton 2014). In contrast, the factors that control IN migration in the developing spinal cord remain almost totally unknown.

In the embryonic spinal cord, distinct neuronal populations are generated from different progenitor domains orderly distributed along the dorsoventral axis of the ventricular zone. These progenitors produce motor neurons and multiple populations of ventral or dorsal INs (Lai, Seal, and Johnson 2016, Lu, Niu, and Alaynick 2015). In contrast to motor neurons, spinal IN populations do not organize into columns along the anteroposterior axis of the spinal cord (Francius et al. 2013). Nevertheless, they each migrate according to a stereotyped pattern and settle down at specific focused or diffuse locations in the spinal parenchyma (Grossmann et al. 2010). Recent studies demonstrated that proper neuronal distribution is critical for adequate formation of spinal circuits. Indeed, the clustering and dorsoventral settling position of motor neuron pools critically pattern sensory input specificity (Surmeli et al. 2011). Position of dorsal INs along the mediolateral axis in lamina V determines their connectivity with sensory afferents (Hilde et al. 2016) while extensor and flexor premotor INs segregate along the medio-lateral axis of the spinal cord (Tripodi, Stepien, and Arber 2011). Positional distinctions among premotor INs additionally correlate with their output to different motor columns (Goetz, Pivetta, and Arber 2015) and differential distribution of V1 IN subsets constrain patterns of input from sensory and from motor neurons (Bikoff et al. 2016). Consistently, distinct ventral IN subsets are differentially distributed along the anteroposterior axis of the spinal cord (Francius et al. 2013, Hayashi et al. 2018) and integrate into specific local microcircuit modules (Hayashi et al. 2018). However, the molecular mechanisms that regulate proper distribution of spinal INs remain elusive.

During their migration, cardinal populations of spinal neurons undergo progressive diversification into distinct subsets that exert specific functions in spinal circuits (Catela, Shin, and Dasen 2015, Lai, Seal, and Johnson 2016, Lu, Niu, and Alaynick 2015). For example, V2 INs diversify into major V2a and V2b and minor V2c and V2d populations. V2a and V2d are excitatory neurons that participate in left-right alternation at high speed and contribute to rhythmic activation of locomotor circuits, respectively (Crone et al. 2008, Dougherty and Kiehn 2010, Dougherty et al. 2013). V2b cells are inhibitory INs that participate in alternation of flexor vs extensor muscle contraction (Britz et al. 2015). As observed for V1 INs (Bikoff et al. 2016), V2 cells further diversify into more discrete subpopulations differentially distributed along the anteroposterior axis of the spinal cord (Francius et al. 2013, Hayashi et al. 2018). However, specific functions of these IN subsets have not been investigated yet, and the mechanisms that govern their production remain currently unknown.

Recently, we identified Onecut (OC) transcription factors as regulators of neuronal diversification (Kabayiza et al. 2017, Roy et al. 2012, Francius and Clotman 2014) and of dorsal IN migration (Kabayiza et al. 2017) in the developing spinal cord. OC factors, namely Hepatocyte Nuclear Factor-6 (HNF-6, or OC-1), OC-2 and OC-3, are transcriptional activators present in the digestive tract and in the CNS during embryonic development (Jacquemin et al. 1999, Lemaigre et al. 1996, Jacquemin et al. 2003, Landry et al. 1997, Vanhorenbeeck et al. 2002). In neural tissue, they regulate production (Espana and Clotman 2012a), diversification (Roy et al. 2012, Francius and Clotman 2014, Kabayiza et al. 2017), distribution (Audouard et al. 2013, Espana and Clotman 2012a, b, Kabayiza et al. 2017) and maintenance (Espana and Clotman 2012a, b, Stam et al. 2012) of specific neuronal populations, as well as the formation of neuromuscular junctions (Audouard et al. 2012). Here, we demonstrate that OC factors regulate the diversification and the distribution of V2 INs during spinal cord development. Analyzes of OC-deficient embryos showed defective production of specific subpopulations of V2a INs, as well as abnormal distribution of V2a and V2b cells in the developing spinal cord. Furthermore, we uncovered that OC proteins act upstream of specific spinal isoforms of Pou2f2, a POU family transcription factor. Using gain- or loss-of-function experiments, we demonstrated that, as observed for OC factors, Pou2f2 regulates the distribution of V2 INs in the developing spinal cord. Thus, we uncovered a genetic pathway that regulates the diversification and the migration of V2 INs during embryonic development.

Results

OC factors are present in multiple subsets of spinal V2 interneurons

In the developing spinal cord, OC factors contribute to diversification, migration and maintenance of different neuronal populations (Kabayiza et al. 2017, Roy et al. 2012, Stam et al. 2012). To study V2 interneuron diversification, we previously established a repertoire of markers that divide embryonic V2 cells into multiple subpopulations (Francius et al. 2013). Although OC factors have been detected in V2 interneurons (Francius and Clotman 2010), their distribution in V2 subsets has not been investigated yet. Therefore, we first determined the presence of each OC in these V2 subpopulations at e12.5.

V2a interneurons include neuronal subsets characterized by the presence of Shox2, MafA, cMaf, Bhlhb5 or Prdm8 (Francius et al. 2013). Only Hnf6 was detected in few Shox2+ V2a cells (Figure 1A-C"; Table 1). In contrast, the 3 OC proteins were detected in MafA+ and cMaf+ V2a subpopulations (Figure 1D-I"; Table 1), but not in Bhlhb5+ or Prdm8+ cells (Table 1; data not shown). V2b interneurons include similar subsets except for Shox2+ and cMaf+ cells, and contain an additional MafB+ subpopulation (Francius et al. 2013). OC were present in MafA+ but not in MafB+, Bhlhb5+ or Prdm8+ V2b subsets (Figure 1J-L"; Table 1; data not shown). In addition, OC were detected in V2c (non-progenitor Sox1+ cells; Figure 1M-O"; Table 1) but not in V2d (Shox2+Chx10-) cells (Figure 1A-C"; Table 1). Thus, OC factors are present in multiple subpopulations of V2 interneurons.

V2 – e12.5				
Populations	**Subpopulations**	**HNF-6**	**OC-2**	**OC-3**
V2a – Chx10		+	+	+
	Shox2	+	-	-
	MafA	+	+	+
	cMaf	+	+	+
	Bhlhb5	-	-	-
	Prdm8	-	-	-
V2b – Gata3		+	+	+
	MafA	+	+	+
	MafB	-	-	-
	Bhlhb5	-	-	-
	Prdm8	-	-	-
V2c – Sox1		+	+	+
V2d – Shox2		-	-	-

Table 1. OC factors are present in specific populations and subpopulations of V2 interneurons. The V2 populations, including V2a, V2b, V2c and V2d, are subdivided in smaller subpopulations characterized by differential expression of transcription factors (Francius et al. 2013). OC factors are detected in specific populations and subpopulations of V2 interneurons.

OC factors regulate the diversification of spinal V2 interneurons

To determine whether OC proteins contribute to the development of V2 interneuron subsets, we characterized the phenotype of these cells in *Hnf6/Oc2* double-mutant embryos, which lack the three OC factors in the developing spinal cord (Kabayiza et al. 2017, Roy et al. 2012). Given that the number and the distribution of cells in each interneuron subpopulation vary along the anteroposterior axis of the spinal cord (Francius et al. 2013, Hayashi et al. 2018, Sweeney et al. 2018), this analysis was systematically performed at brachial, thoracic and lumbar levels at e12.5 and e14.5.

In the absence of OC factors, the total number of Chx10+ interneurons was not significantly changed (Figure 2A-D; Supplementary Figure S1A-B), although a trend toward reduction was detected at brachial level at e12.5 (Figure 2C). A large subset of V2a cells contains Shox2 (Figure 1A-C"; 2E-F"; (Dougherty et al. 2013)). Consistently, the number of Chx10+Shox2+ interneurons was not changed in the absence of OC proteins (Figure 2E-H; Supplementary Figure S1C-D"). These observations suggest that OC are not necessary for V2a interneuron production. In contrast, the smaller V2a subpopulations wherein OC factors were detected in control embryos, characterized by the presence of MafA (Figure 1D-F") or cMaf (Figure 1G-I"), were almost completely lost in OC mutant embryos (Figure 2I-P; Supplementary Figure S1E-H"). As the total number of Chx10+ and of Shox2+ V2a was not changed (Figure 2A-H; Supplementary Figure S1A-D"), the loss of the MafA+ or cMaf+ subsets may be compensated for by expansion of other V2a subpopulations. However, we were unable to detect expansion of any alternative V2a subset (data not shown), suggesting that the absence of OC proteins favor differentiation of V2a subpopulations that remain to be identified. Nevertheless, our data indicate that OC factors are required either for the expression of V2 subpopulation markers or for the differentiation of specific V2a interneuron subsets.

To discriminate between these possibilities and to evaluate the contribution of OC factors to V2b diversification, we characterized the phenotype of V2b interneurons and of their MafA+ subpopulation in the absence of OC proteins. As observed for V2a interneurons, the total number of V2b cells was not changed in OC mutant embryos (Figure 2Q-T; Supplementary Figure S1I-J), although a trend toward reduction was observed at brachial level at e12.5 (Figure 2S). As for V2a, OC are present in the MafA+ V2b subpopulation (Figure 1J-L"). However, in contrast to V2a, the MafA+ V2b interneurons were present in normal number in OC mutant embryos (Figure 2U-X; Supplementary Figure S1K-L''). Hence, OC factors are not necessary for *MafA* expression in spinal V2 interneurons nor for the production of the MafA+ V2b subset, although they are required for the differentiation of the MafA+ and of the cMaf+ V2a subpopulations.

Finally, we assessed the requirement for OC in the production of V2c interneurons, a V2 population strongly related to V2b cells (Panayi et al. 2010) wherein OC are broadly present (Figure 1M-O"). Although weak production of Sox1 in spinal progenitors was preserved, V2c cells characterized by high Sox1 levels were scarcely detectable in OC mutant embryos at

e12.5 (arrows in Figure 2Y-AA). However, the number of V2c was normal at e14.5 (Figure 2BB; Supplementary Figure S1M-N), suggesting that the absence of OC delays the differentiation of V2c interneurons without affecting the V2b population. Taken together, these observations demonstrate that OC proteins are not required for V2 interneuron production but regulate the diversification of V2 interneurons into multiple subpopulations.

OC factors regulate the distribution of spinal V2 interneurons

Although the total number of V2a or V2b interneurons was not affected by the absence of OC factors, careful examination of immunofluorescence labelings suggested that, as observed for spinal dorsal interneurons (Kabayiza et al. 2017), OC proteins may regulate the distribution of V2 interneurons in the developing spinal cord (Figure 2A-B; Q-R). Therefore, quantitative distribution analyses (Kabayiza et al. 2017) were performed for each V2 population present in OC mutant embryos at brachial, thoracic or lumbar levels at e12.5, namely in the course of ventral interneuron migration, and at e14.5, i.e. when ventral interneuron migration in the transverse plane of the spinal cord is completed.

At e12.5 in control embryos, V2a interneurons distributed in 2 connected clusters, a major central group and a minor medial group, at each level of the spinal cord. In mutant embryos, V2a cells similarly distributed in connected central and medial groups. However, the relative cell distribution between the 2 clusters seemed altered, with less central cells at brachial level and less medial cells at lumbar levels (Figure 3A-L). Altered V2a distribution on the mediolateral axis was confirmed at e14.5. In control embryos, the 2 V2a groups did coalesce in a more evenly-distributed population that occupied ~70% of the medio-lateral axis. In mutant embryos, V2a interneurons remained segregated into 2 distinct, although connected, clusters with a majority of cells in medial position (Figure 3M-X). Thus, absence of OC factors perturbs proper distribution of the V2a interneurons and restricts at e14.5 migration of a fraction of V2a cells in a medial position. To assess whether these distribution defects may only affect V2a subsets or impact the whole V2a population, we sought to characterize the distribution of V2a subpopulations. However, the MafA+ and cMaf+ subsets were absent in OC mutants. Therefore, only the broader Shox2+ subpopulation was analyzed. Similar observations were made as for the whole V2a population (Figure 3Y-VV), confirming that absence of OC factors alters the distribution of V2a interneurons.

To assess whether OC also regulate the position of other V2 populations, we studied the distribution of V2b interneurons. At e12.5 in control embryos, V2b cells distributed in a major central (brachial level) or lateral (thoracic and lumbar levels) cluster with minor subsets located more medially (arrows in Figure 4A-L) or ventrally (arrowheads in Figure 4A-L). In OC mutant embryos at e12.5, the major population was more compact, more centrally located and slightly more ventral. In addition, the ventral V2b subset was significantly depleted (asterisks in Figure 4A-L). Consistently, at e14.5, V2b interneurons in the central cluster remained significantly more compact at brachial level in the absence of OC factors, and identical trends were observed at thoracic and lumbar levels (Figure 4M-X). In addition, a small contingent of V2b migrating towards the medio-dorsal spinal cord in control embryos (arrowheads in Figure 4M-X) was missing in OC mutant littermates (asterisks in Figure 4M-X). Thus, as observed for V2a cells, absence of OC factors perturbs proper distribution of the V2b interneurons. The MafA+ V2b subset was too small to enable reliable distribution analysis. Taken together, these observations demonstrate that, in addition to V2 diversification, the OC transcription factors regulate proper distribution of V2 interneurons during spinal cord development.

OC factors control expression of neuronal-specific isoforms of *Pou2f2*

In an effort to identify genes downstream of OC that may contribute to V2 interneuron differentiation and distribution, we performed a microarray comparison of control and of OC-deficient spinal cord transcriptome at e11.5, namely at the stage when significant numbers of V2 cells have been generated and are initiating migration. Among genes showing a differential expression level in the OC mutant spinal cord, *Pou2f2* was significantly upregulated (1.57-fold increase). Pou2f2 (previously named Oct-2) is a transcription factor containing a POU-specific domain and a POU-type homeodomain (Figure 5A) that binds an octamer motif (consensus sequence ATGCAAAT) (Latchman 1996). *Pou2f2* expression has been detected in B lymphocytes, in neuronal cell lines and in neural tissues including the developing CNS (Lillycrop and Latchman 1992, Camos et al. 2014, Hatzopoulos et al. 1990). Pou2f2 is required for differentiation of B lymphocytes and for postnatal survival (Corcoran et al. 1993, Corcoran et al. 2004, Hodson et al. 2016, Konig et al. 1995), and is able to modulate neuronal differentiation of ES cells (Theodorou et al. 2009). However, its role in the developing spinal cord remains unknown.

Based on work in B cells, multiple *Pou2f2* isoforms generated by alternative splicing have been described (Figure 5A; (Lillycrop and Latchman 1992, Wirth et al. 1991, Hatzopoulos et al. 1990, Liu, Lillycrop, and Latchman 1995, Stoykova et al. 1992)). Therefore, we first determined whether similar isoforms are found in the developing spinal cord. However, using RT-PCR experiments, we systematically failed to obtain PCR products using upstream primers in described exon 1 (asterisks in Supplementary Figure S2A-B and data not shown; Table 2) and amplifications encompassing exons 5 to 6 generated predominant amplicons larger than expected (arrowheads in Supplementary Figure S2B; Table 2), suggesting the existence of alternative exons in *Pou2f2* embryonic spinal cord transcripts (Figure 5A). Data mining the NCBI Nucleotide database for *Pou2f2* sequences identified a predicted murine *Pou2f2* isoforms (X6 sequence, accession number XM_006539651.3) with a different exon 1 (E1X) and an additional sequence between exons 5 and 6, the size of which (279 bp) corresponded to the size differences estimated in our amplifications encompassing exons 5 to 6 (arrowheads in Supplementary Figure S2B; Table 2). Using PCR primers in this predicted sequence, we were able to amplify a 5' region of *Pou2f2* from the alternative E1X exon and an additional sequence between exons 5 and 6 (Supplementary Figure S2C; Table 2), suggesting that alternative isoforms similar to this predicted sequence are produced in the developing spinal cord. However, amplifications from E1X systematically produced 2 amplicons (arrowheads in Supplementary Figure S2C; Table 2), suggesting the existence of an alternative exon downstream to E1X. Sequencing of our PCR products and alignment to genomic DNA confirmed that predominant *Pou2f2* isoforms in the developing spinal cord contain the alternative E1X exon, an additional exon (E5b) between exons 5 and 6, and can undergo alternative splicing of a short (61bp) exon (E1b) between E1X and exon 2 (Supplementary Figure S2D). E5b exon maintains the reading frame. In contrast E1b exon disrupts the reading frame, imposing the use of the ATG located in exon 2 to generate a functional Pou2f2 protein, whereas the absence of E1b leaves open the use of an alternative upstream ATG located at the 3' end of E1X (Figure 5A; Supplementary Figure S2D). Hence, taking into account our RT-PCR and sequencing data, 4 neuronal *Pou2f2* isoforms that are different from the previously described B-cell or neural isoforms can be produced in the developing spinal cord (Fig 5A).

However, our RT-PCR experiments suggested that minor transcripts corresponding to B-cell isoforms are also present in the embryonic spinal cord (Supplementary Figure S2A-B; Table

2). To assess the relative abundance of each transcript type in this tissue and to evaluate the extent of their relative overexpression in the absence of OC factors, we quantified each isoform type in control and in OC-deficient spinal cord at e11.5. In control spinal cords, spinal *Pou2f2* isoforms were >30-fold more abundant than B-cell isoforms (Figure 5B), consistent with our RT-PCR observations (Supplementary Figure S2). In the absence of OC factors, spinal isoforms were ~2.6-fold overexpressed whereas B-cell isoforms barely trended to increase (Figure 5C-D), resulting in spinal isoforms being >60-fold more abundant than B-cell transcripts (Figure 5E). Thus, OC factors repress expression of spinal *Pou2f2* isoforms in the developing spinal cord.

To confirm these data and to determine the expression pattern of *Pou2f2* in the ventral spinal cord, *in situ* hybridization was performed on sections from control or *Hnf6/Oc2* double-mutant spinal cords using either a generic *Pou2f2* probe complementary to spinal and to B-cell isoforms or a spinal isoform-specific probe corresponding only to exon E5b (Figure 5A). Using the generic *Pou2f2* probe on control tissue, we detected *Pou2f2* transcripts in the ventral region of the spinal cord, with lower expression levels in the location of the motor columns (arrows in Figure 5F). In OC mutant embryos, *Pou2f2* expression was globally increased and additionally expanded in the ventral area (arrowheads in Figure 5F-G) including the motor neuron territories (arrows in Figure 5F-G). Similar observations were made with the spinal-specific probe, although the signal was much weaker probably owing to the shorter length of the probe (Figure 5H-I). Thus, OC factors restrict and moderate *Pou2f2* expression in ventral spinal populations likely including V2 interneurons.

Amplification	Expected sizes	B cells	Control spinal cord
E1 → E6	272 bp 390 bp 456 bp	272 bp 390 bp 456 bp	No amplification
E7 → E9	174 bp 222 bp	174 bp 222 bp	174 bp
E10 → E12	452 bp	452 bp	452 bp
E13 → E17	160 bp 296 bp 370 bp	160 bp 296 bp 370 bp	370 bp
E1 → E7	348bp 466 bp 532 bp	466 bp 532 bp	No amplification
E2 → E7	284 bp 402 bp 468 bp	402 bp 468 bp	~ 680 bp ~ 750 bp
E3 → E6	154 bp 272 bp 378 bp	154 bp 272 bp 378 bp	272 bp 378 bp ~ 550 bp ~ 600 bp
E4 → E7	340 bp	340 bp	~ 600 bp
E5 → E7	201 bp	201 bp	201 bp ~ 460 bp
E6 → E7	160 bp	160 bp	160 bp
E1X → E3	152 bp	No amplification	152 bp ~ 220 bp
E1X → E5b	554 bp 620 bp	N.D	554 bp 620 bp
E5b	234 bp	N.D	234 bp
E3 → E5b	429 bp 495 bp	N.D	429 bp 495 bp
E5b → E7	416 bp	N.D	416 bp

Table 2. *Pou2f2* isoforms in the developing spinal cord are different from B-cell isoforms. Regions covering B lymphocytes or predicted *Pou2f2* isoforms (exons E1 or E1X to E17) were amplified by RT-PCR from B lymphocyte or embryonic spinal cord RNA. Orange cells = unexpected results.

Pou2f2-positive V2 interneurons are mislocated in the absence of OC factors

To assess whether increased *Pou2f2* expression in *Hnf6*$^{-/-}$;*Oc2*$^{-/-}$ spinal cords corresponded to an expansion of Pou2f2 distribution in V2 interneurons or an upregulation in its endogenous expression territory, we first quantified the number and distribution of Pou2f2-containing Chx10+ cells at e12.5 and e14.5 (Figure 6; Supplementary Figure S3). Immunofluorescence experiments demonstrated that Pou2f2 is present in V2a interneurons in control embryos (Figure 6A,C; Supplementary Figure S3A,D). They also confirmed increased Pou2f2 production in the ventral regions of the spinal cord in OC mutant embryos (Figure 6A-F). However, the increase in Pou2f2-positive V2a interneurons was not statistically significant (Figure 6E-F; Supplementary Figure S3). This suggested that, in the absence of OC factors, *Pou2f2* is upregulated but only modestly expanded in the V2a population. In contrast, the distribution of Pou2f2-positive V2a interneurons was affected (Figure 6A-D, 6G-DD). At e12.5, cells in the central clusters were slightly reduced at brachial and at thoracic levels (Figure 6G-R). In contrast, at e14.5, a majority of V2a containing Pou2f2 settled in a medial position (Figure 6S-DD), reminiscent of the distribution defects observed for the whole V2a population (Figure 3). Similarly, Pou2f2 was detected in V2b interneurons in control embryos, although in a more restricted number of cells (Figure 7A-F). In the absence of OC factors, the number of Pou2f2-positive V2b cells was not significantly increased (Figure 7E-F) but, as observed for V2a, this subset of V2b interneurons was slightly mislocated with cells more central at e12.5 and more clustered on the medio-lateral axis at e14.5 (Figure 7G-DD). Taken together, these observations suggest that Pou2f2 may contribute to control V2 interneuron migration during spinal cord development and that increased *Pou2f2* expression in these cells could participate in alterations of V2 distribution in the absence of OC factors.

Pou2f2 regulates the distribution of spinal V2 interneurons

To determine whether Pou2f2 is able to modulate V2 interneuron distribution, we expressed *Pou2f2*, which is not present in the chicken genome (data not shown), in the chicken embryonic spinal cord (Supplementary Figure S4). Pou2f2 did not impact on the number of V2a, Shox2-containing V2a, V2b or V2d interneurons (Figure 8A-B", 8K-P). In contrast, it did alter V2 interneuron location. In HH27-28 control spinal cord, V2a and Shox2-containing V2a interneurons were distributed in 2 closely connected clusters on the medio-lateral axis of the neuroepithelium. In electroporated spinal cord, lateral migration was increased and a majority of V2a and Shox2-positive V2a interneurons were clustered in a single group in a central position (Figure 8A-J) with ectopic lateral extensions (arrows in Figure 8D,H). In control spinal cord, V2b were distributed in 2 groups along the medio-lateral axis with a majority of cells in the lateral cluster. In electroporated spinal cord, lateral migration of the V2b interneurons was reduced and a majority of cells were located in the medial cluster (Figure 8O-T). Thus, consistent with our observation in OC mutant embryos, increased Pou2f2 seems to modulate migration of V2 interneurons in the developing spinal cord.

To confirm the influence of Pou2f2 on V2 migration, we studied V2 distribution in mouse embryos devoid of Pou2f2 (Corcoran et al. 1993) at e12.5. Absence of Pou2f2 did not impact on the number of V2a, Shox2-positive V2a or V2d interneurons (Figure 9A-G) nor on the cMaf+ or Maf+ V2a subsets (Supplementary Figure S5). In contrast, V2a distribution was affected in *Pou2f2* mutants. As compared to the two V2a clusters observed in control embryos, Chx10+ cells were relatively more abundant in the medial cluster in *Pou2f2* mutant embryos (Figure 9H-S). Similarly, Shox2+ V2a remained more medial at brachial level, but migrated more laterally at lumbar level (Figure 9T-EE). Consistent observations were made for V2b and V2c interneurons (Figure 10). Although the number of V2b, V2c or MafA+ V2b cells was not changed in the absence of Pou2f2 (Figure 10A-C; Supplementary Figure S6), V2b cells remained more medial at thoracic levels but migrated more laterally at lumbar levels (Figure 10D-O). Taken together, these observations demonstrate that Pou2f2 regulate the distribution of V2 interneurons during spinal cord development.

Discussion

In the recent years, several studies demonstrated that proper distribution of neuronal populations and subpopulations in the developing spinal cord is critical for adequate formation of spinal circuits (Bikoff et al. 2016, Goetz, Pivetta, and Arber 2015, Hayashi et al. 2018, Hilde et al. 2016, Surmeli et al. 2011, Tripodi, Stepien, and Arber 2011). However, the genetic programs that control the diversification of spinal neuronal populations into specialized subpopulations and the proper settling of these neuronal subsets in the spinal parenchyma remain elusive. Here, we provide evidence that OC transcription factors regulate the diversification of spinal V2 INs, and that a genetic cascade involving OC factors and their downstream target Pou2f2 controls the distribution of V2 INs in the developing spinal cord.

Control of V2 IN diversification by the OC factors

Cardinal populations of spinal ventral INs have been well characterized, and their global contribution to the activity of motor circuits has been extensively studied (reviewed in (Boije and Kullander 2018, Gosgnach et al. 2017, Ziskind-Conhaim and Hochman 2017). However, more recently, the idea emerged that these cardinal populations are not homogeneous ensembles but rather contain multiple cellular subsets with distinct molecular identities and functional properties. V0 INs are constituted of two major populations, the inhibitory $V0_D$ and the excitatory $V0_V$ neurons, which control left-right alternation of motor circuit activation at low or high frequencies, respectively (Talpalar et al. 2013). V1 INs, a major inhibitory population that controls motor output, can be fractionated into ~50 distinct subsets based on the combinatorial expression of 19 transcription factors. These subsets exhibit distinct electrophysiological properties and highly structured spatial distribution that constraints somato-sensory afferences (Bikoff et al. 2016). Furthermore, they are differentially distributed along the anteroposterior axis of the spinal cord (Francius et al. 2013, Sweeney et al. 2018), suggesting differential contribution to the motor output at thoracic or at limb levels of the spinal cord (Sweeney et al. 2018). Similarly, V2a INs comprise two major divisions, namely type I and type II V2a cells, that are arrayed in counter-gradients along the antero-posterior axis of the spinal cord and activate different patterns of motor output at brachial and lumbar levels. Furthermore, these two large divisions can themselves

be fractionated at birth into 11 subsets characterized by distinct combinations of markers, differential segmental localization and specific distribution patterns on the medio-lateral axis of the spinal cord (Hayashi et al. 2018). In the zebrafish, 3 distinct subclasses of V2a INs participate in separate microcircuit modules driving slow, intermediate or fast motor neuron activity (Ampatzis et al. 2014). Finally, V3 INs segregate into physiologically and topographically distinct clusters along the dorso-ventral axis of the spinal cord, each showing distinctive maturation processes and likely playing different roles in motor activity (Borowska et al. 2015, Borowska et al. 2013). Taken together, these observations suggest that cardinal IN populations only constitute the first organization level of functionally distinct neuronal subsets that contribute to diversity and flexibility within spinal motor circuits. We show here that, as observed in spinal motor neurons and other IN populations (Francius and Clotman 2010, Francius et al. 2013, Kabayiza et al. 2017), OC factors are also detected in subsets of V2 INs. As reported for the V1 population (Bikoff et al. 2016, Sweeney et al. 2018), OC proteins may define functionally-relevant V2 subpopulations, although possible correlation with the recently-identified V2a subsets (Hayashi et al. 2018) remains to be investigated.

However, for each of these cardinal populations, the genetic programs that contribute to their diversification into multiple subpopulations remain unknown. Our observations demonstrate that OC factors contribute to the diversification of V2 INs. Normal numbers of cardinal V2a and V2b cells were generated in OC mutant embryos, suggesting that these factors do not contribute to the production of V2 cells (Clovis et al. 2016, Lee et al. 2008, Thaler et al. 2002) nor to the segregation of the V2a and V2b lineages through differential activation of Notch signaling (Del Barrio et al. 2007, Joshi et al. 2009, Misra et al. 2014, Peng et al. 2007). In contrast, V2a subpopulations characterized by the presence of MafA or cMaf were strongly depleted in the absence of OC proteins. Uncomplete knowledge of the whole collection of V2a subsets prevented to assess whether this reduction in specific subpopulations were compensated for by an expansion of neighboring subsets. Furthermore, MafA and cMaf were not included among the markers that fractionate at birth the V2a population into 11 distinct subgroups (Hayashi et al. 2018) and the matching between these subpopulations therefore remains to be investigated. Nevertheless, these observations suggest that, as previously observed for spinal motor neurons (Roy et al. 2012) and dorsal INs (Kabayiza et al. 2017), OC factors contribute to the diversification of V2a INs

during development. In addition, the production of V2c cells was delayed in OC mutant embryos, although V2b that are supposed to constitute the source of V2c (Panayi et al. 2010) were timely generated. This points to a specific contribution of OC protein to the development of V2c INs, the mechanism of which is currently unknown.

Control of V2 IN migration by the OC factors

Beside diversification, the characterization of functionally distinct IN subpopulations unveiled a strong correlation between the distribution of each IN subset and their contribution to distinct microcircuit modules. Extensor and flexor premotor INs segregate along the medio-lateral axis of the spinal cord (Tripodi, Stepien, and Arber 2011). Premotor INs that convey information to motor neurons innervating axial muscles reside in symmetrically balanced locations while limb-innervating motor neurons are mainly innervated by ipsilateral premotor INs (Goetz, Pivetta, and Arber 2015). The settling position of distinct V1 IN subsets is predictive of the status of motor and sensory neuron input (Bikoff et al. 2016). Among V2 INs, type I cells are distributed as an increasing rostro-caudal gradient and contribute to local motor circuits, whereas type II cells are arrayed as an increasing caudo-rostral gradient and project both to motor neurons and supraspinally (Hayashi et al. 2018), likely sending motor efference copies to the cerebellum via the lateral reticular nucleus (Azim et al. 2014, Pivetta et al. 2014). Furthermore, ventral and dorsal V3 INs are differentially activated during running and swimming, suggesting specific contribution of spatially distinct V3 subsets to different motor behavior (Borowska et al. 2013). Finally, inhibitory sensory relay neurons of lamina V characterized by the presence of SATB2 are abnormally located upon *SATB2* inactivation and this, along with changes in molecular identity, perturbs pre- and post-synaptic connectivity (Hilde et al. 2016). Taken together, these recent data support a model wherein correct localization of spinal IN subsets is critical for proper formation of sensory and sensory-motor circuits, reminiscent of the requirement of correct motor neuron positioning for the establishment of adequate sensory inputs (Surmeli et al. 2011, Dasen 2017). This highlights the importance of a strict regulation of short-distance neuronal migration in the developing spinal cord.

However, genetic determinants that control spinal IN migration have only been sparsely identified. Sim1 regulate ventro-dorsal migration of the V3 IN subsets (Blacklaws et al. 2015). Similarly, SATB2 control the position of inhibitory sensory relay INs along the medio-lateral

axis of the spinal cord (Hilde et al. 2016). Here, we provide evidence that the OC factors control a genetic program that regulates proper positioning of V2 INs during embryonic development. In the absence of OC proteins, a fraction of V2a INs remained in a more medial location, expanding the medial cluster containing locally-projecting cells at the expanse of the lateral cluster that comprises the supraspinal-projecting V2a INs (Hayashi et al. 2018). V2b alterations were less spectacular, although ventral and dorsal contingents were reduced and the cell distribution in the central cluster was altered. Variability in the alterations observed at e12.5 and e14.5 suggests that, depending on the population considered, migration of earlier- or later-migrating neurons may be differently affected by the absence of OC proteins. Functional distinctions between V2b subsets have not been reported to date. However, given our current knowledge regarding the diversification and the impact of localization of V1 and V2a IN subpopulations on proper circuit formation (Bikoff et al. 2016, Hayashi et al. 2018), we hypothesize that even slight perturbations in the distribution of small IN subsets are likely to result in alterations in spinal microcircuit development. Our observations are consistent with the contribution of OC factors to the migration of several populations of spinal dorsal INs (Kabayiza et al. 2017). This raises the question whether similar cues might be regulated by identical genetic programs and used by different IN populations to organize proper distribution of ventral and dorsal IN subsets in the developing spinal cord. Identification of the factors downstream of OC protein involved in the control of neuronal migration will be necessary to answer this question.

A OC-Pou2f2 genetic cascade regulates the migration of V2 INs

Therefore, we attempted to identify genes downstream of OC factors and possibly involved in the control of IN migration using a global approach comparing the transcriptome of whole spinal cords isolated from control or OC-deficient embryos. However, we were unable to detect significant changes in the expression of known regulators of neuronal migration. This suggests that different actors may be active downstream of OC proteins in distinct IN subsets to regulate proper neuronal distribution. In contrast, we uncovered that expression of the transcriptional regulator *Pou2f2* is repressed by OC factors in multiple IN populations. Surprisingly, our data demonstrated that variant *Pou2f2* isoforms are produced in the developing spinal cord as compared to B lymphocytes (Lillycrop and Latchman 1992, Wirth et al. 1991, Hatzopoulos et al. 1990, Liu, Lillycrop, and Latchman 1995, Stoykova et al. 1992),

and that these spinal variants are regulated by OC proteins. Spinal-enriched transcripts encode Pou2f2 proteins containing additional peptidic sequences upstream of the POU-specific domain and of the homeodomain. Furthermore, exon 1 is different and corresponds to sequences located ~47kb upstream of the transcription initiation site used in B cells (data not shown) in the mouse genome, suggesting that OC regulate *Pou2f2* expression from an alternative promoter. However, we cannot exclude that additional exon(s) could be present upstream of the identified sequences, and determination of the regulating sequences targeted by the OC protein will require thorough characterization of the produced transcripts. In addition, we cannot rule out indirect regulation of *Pou2f2* expression by the OC factors, as these proteins are usually considered to be transcriptional activators rather than repressors (Beaudry et al. 2006, Jacquemin et al. 2000, Jacquemin, Lemaigre, and Rousseau 2003, Lannoy et al. 2000, Pierreux et al. 2004, Roy et al. 2012). Whether divergent N-terminal sequence and additional peptidic sequence upstream of the POU-specific domain modifies the activity or the binding specificity of the Pou2f2 proteins also awaits further investigations.

Nevertheless, our observations demonstrate that Pou2f2 is downstream of OC factors in the V2 INs and also contributes to regulate the distribution of V2 INs during embryonic development. The number of Pou2f2-containing V2 was not significantly increased in OC mutant spinal cords, suggesting that the absence of OC protein resulted in derepression of Pou2f2 production in its endogenous expression domain rather that ectopic activation in other V2 subsets. Increased production of Pou2f2 in the chicken embryonic spinal cord resulted in alterations in the localization of V2 populations without any change in cell number, pointing to a possible contribution of Pou2f2 to the regulation of V2 migration downstream of OC factors. Consistently, V2 distribution was perturbed in *Pou2f2* mutant embryos without any alteration in V2 population or subpopulation cell numbers, demonstrating the involvement of Pou2f2 in the control of V2 IN distribution. Hence, we uncovered a genetic cascade comprising OC and Pou2f2 transcription factors that ensures proper migration of V2 cells during spinal cord development. This program may not be restricted to V2 cells, as diversification and distribution of dorsal INs and of motor neurons are also altered in the absence of OC factors (Kabayiza et al. 2017, Roy et al. 2012) and as *Pou2f2* expression in the OC mutant spinal cord is increased in multiple neuronal populations (Figure 5D-I). Therefore, evaluating the consequences of V2 IN defects on motor

circuit activity in *OC* or *Pou2f2* mutants would necessitate conditional inactivation of these transcription factors in this specific population. Whether V2 localization defects are associated with axon guidance perturbations, as observed for V3 INs in the absence of Sim1 (Blacklaws et al. 2015), will require genetic labeling of V2 axonal projections.

Localization defects of specific neuronal populations have previously been reported in the absence of OC factors. Dopaminergic neurons of the A13 nucleus migrate aberrantly in OC mutant embryos, resulting in the disaggregation of the nucleus and loss of dopaminergic cell phenotype (Espana and Clotman 2012b). Similarly, neurons of the Locus Coeruleus, the largest noradrenergic nucleus of the CNS, migrate caudally beyond their normal position in the rostral hindbrain of OC deficient individuals, resulting in the loss of their catecholaminergic characteristics (Espana and Clotman 2012a). Final positioning of the Purkinje cells during postnatal maturation of the cerebellum was defective in the absence of HNF-6 (Audouard et al. 2013). Finally, distribution defects of spinal dorsal INs in OC mutant embryos have recently been reported (Kabayiza et al. 2017). Hence, OC factors seem critical for proper localization of multiple neuronal populations throughout the CNS. Whether identical migration regulators are controlled by OC proteins in different neuronal populations remains to be determined. Comparison of downstream targets of OC and of Pou2f2 that would be oppositely regulated in the respective mutants may constitute a strategy to identify these regulators.

Materials and methods

Ethics statement and mouse lines

All experiments were strictly performed in accordance with the European Community Council directive of 24 November 1986 (86-609/ECC) and the decree of 20 October 1987 (87-848/EEC). Mice were raised in our animal facilities and treated according to the principles of laboratory animal care, and experiments and mouse housing were approved by the Animal Welfare Committee of Université catholique de Louvain (Permit Number: 2013/UCL/MD/11 and 2017/UCL/MD/008). The day of vaginal plug was considered to be embryonic day (e) 0.5. A minimum of three embryos of the same genotype was analyzed in each experiment. The embryos were collected at e12.5 and e14.5. The *Hnf6;Oc2* and the *Pou2f2* mutant mice were previously described (Clotman et al. 2005, Corcoran et al. 1993, Jacquemin et al. 2000). The mice and the embryos were genotyped by PCR (primer information available on request).

In situ hybridization (ISH) and immunofluorescence labelings

For ISH, the collected embryos were fixed in ice-cold 4% paraformaldehyde (PFA) in phosphate buffered-saline (PBS) overnight at 4°C, washed thrice in PBS for 10 minutes, incubated in PBS/30% sucrose solution overnight at 4°C, embedded and frozen in PBS/15% sucrose/7.5% gelatin. Fourteen µm section were prepared and ISH was performed as previously described (Beguin et al. 2013, Francius et al. 2016, Pelosi et al. 2014) with DIG-conjugated Pou2f2 (NM_011138.1, nucleotides 604-1187) or Pou2f2 exon 5b (XM_006539651.3, nucleotides 643-876) antisense RNA probes.

For immunofluorescence, collected embryos were fixed in 4% PFA/PBS for 25 or 35 minutes according to their embryonic stage and processed as for ISH. Immunolabeling was performed on 14 µm serial cryosections as previously described (Francius and Clotman 2010). Primary antibodies against the following proteins were used: Chx10 (sheep; 1:500; Exalpha Biologicals #X1179P), Foxp1 (goat; 1:1000; R&D Systems #AF4534), Gata3 (rat; 1:50; Absea Biotechnology #111214D02), GFP (chick; 1:1000; Aves Lab #GFP-1020), HNF6 (guinea pig; 1:2000; (Espana and Clotman 2012b); or rabbit; 1:100; Santa Cruz #sc-13050; or sheep; 1:1000 R&D Systems #AF6277), cMaf (rabbit; 1:3000; kindly provided by H. Wende), MafA (guinea pig; 1:500; kindly provide by T. Müller), OC2 (rat; 1:400; (Clotman et al. 2005); or

585 sheep; 1:500; R&D Systems #AF6294), OC3 (guinea pig; 1:6000; (Pierreux et al. 2004)),
586 Pou2f2 (rabbit; 1:2000; Abcam #ab178679), Shox2 (mouse; 1:500; Abcam #ab55740), Sox1
587 (goat; 1:500; Santa Cruz #sc-17318). Secondary antibodies donkey anti-guinea
588 pig/AlexaFluor 488, 594 or 647, anti-mouse/AlexaFluor 488, 594 or 647, anti-
589 rabbit/AlexaFluor 594 or 647, anti-goat/AlexaFluor 488, anti-rat/AlexaFluor 647, anti-
590 sheep/AlexaFluor 594 or 647, and goat anti-mouse IgG2A specific/AlexiaFluor 488,
591 purchased from ThermoFisher Scientific or Jackson Laboratories were used at dilution
592 1:2000 or 1:1000, respectively.
593
594 ***In ovo* electroporation**
595 *In ovo* electroporations were performed at stage HH14-16, as previously described (Roy et
596 al. 2012). The coding sequence of the S_Pou2f2.4 transcript was amplified by overlapping-
597 PCR using: forward 5' GCTCTGTCTGCCCAAGAGAAA 3' and reverse 5'
598 GTTGGGACAAGGTGAGCTGT 3' primers for the 5' sequence, forward 5'
599 CCACCATCACAGCCTACCAG 3' and reverse 5' ATTATCTCGAGCCAGCCTCCTTACCCTCTCT 3'
600 (designed to enable integration at the *Xho*I restriction site of the pCMV-MCS vector) primers
601 for the 3' sequence. This sequence was first subcloned in a pCR®II-Topo® vector (Life
602 Technologies, 45-0640) for sequencing then subcloned at the *Eco*RI (from the pCR®II-Topo®
603 vector) and *Xho*I restriction sites of a pCMV-MCS vector for the *in ovo* electroporation. The
604 pCMV-Pou2f2 (0.5 μg/μl) vector was co-electroporated with a pCMV-eGFP plasmid
605 (0.25μg/μl) to visualize electroporated cells. The embryos were collected 72 hours (HH27-
606 28) after electroporation, fixed in PBS/4%PFA for 45 minutes and processed for
607 immunofluorescence labelings as previously described (Francius and Clotman 2010).
608
609 **Imaging and quantitative analyses**
610 Immunofluorescence and ISH images of cryosections were acquired on an EVOS FL Auto
611 Imaging System (Thermo Fisher Scientific) or a Confocal laser Scanning biological microscope
612 FV1000 Fluoview with the FV10-ASW 01.02 software (Olympus). The images were processed
613 with Adobe Photoshop CS5 software to match brightness and contrast with the observation.
614 Quantifications were performed on red or green or blue layer of acquired confocal images
615 and double or triple labeled cells were processed by subtractive method (Francius and
616 Clotman 2010). For each embryo ($n \geq 3$), one side of three to five sections at brachial,

thoracic or lumbar level were quantified using the count analysis tool of Adobe Photoshop CS5 software. Raw data were exported from Adobe Photoshop CS5 software to Sigma Plotv12.3 software to perform statistical analyses. The histograms were drawn with Microsoft Excel. Adequate statistical tests were applied based on the number of comparisons and on the variance in each group. For analysis of cell quantifications based on comparison of two groups (control or mutant), standard Student's *t*-tests or Mann-Whitney U tests were performed. Quantitative analyses were considered significant at $p \leq 0.05$ (Three asterisks (***) indicate $p \leq 0.001$).

Quantitative analyzes of interneuron spatial distribution were performed as previously described (Kabayiza et al. 2017). Statistical analyses of ventral IN distribution were performed using a two-sample Hotelling's T2, which is a two-dimensional generalization of the Student's t test. The analysis was implemented using the NCSS software package.

Microarray analyses

RNA was extracted from control or *Hnf6/Oc2* double-mutant spinal cords. The tissue was manually dissociated in Tripur isolation reagent (Roche, 11 667 165 001). After dissociation, chloroform (Merck Millipore, 1 02445 1000) was added to the sample, incubated at room temperature for 10 minutes and centrifugated for 10 minutes at 4°C. The aqueous phase was collected and the RNA was precipitated with isopropanol (VWR, 20880.310) and centrifugated for 15 minutes at 4°C. The pellet was washed in ethanol (Biosolve, 06250502) and centrifugated for 10 minutes at 4°C. The dried pellet was resuspended in RNAse free water. The integrity of the RNA was assessed using an Agilent RNA 6000 Nano assay procedure. For microarray analyzes, the RNA was converted in single-strand cDNA, labeled using the GeneChip® WT PLUS Reagent Kit (Affymetrix) and hybridized on the GeneChip® MoGene 2.0 ST array (Affymetrix, 90 2118) using Affymetrix devices: Genechip ® Fluidics Station 450, Genechip® Hybridization oven 640, Affymetrix Genechip® scanner and the Expression Consol software. The analyzes were performed using the R software. Microarray data have been deposited in the GEO repository (accession number: GSE117871).

Amplification of *Pou2f2* isoforms and sequencing

Fragments of the different *Pou2f2* isoforms were amplified by RT-PCR from RNA of control B lymphocytes or embryonic spinal cords purified as described above. cDNA was obtained

649 from 500 ng of RNA using the iScript™ Reverse transcriptase and the 5x iScript™ reaction
650 mix (BioRad). Conserved or divergent sequences of *Pou2f2* isoforms were amplified as
651 shown in Table 2 using a GoTaq® Green master mix (Promega, M712) or a Q5® Hot Start
652 High-Fidelity DNA Polymerase (New England BioLabs® Inc, M0493S) (primer information
653 available on request). Sequencing of the spinal *Pou2f2* exons was outsourced to Genewiz.
654 For quantitative RT-PCR, RNA was extracted from control (n = 5) or Hnf6/Oc2 double-mutant
655 (n = 4) spinal cords and purified and retrotranscribed as described above. Quantitative real-
656 time PCR was performed on 1/100 of the retrotranscription reaction using iTaq™ universal
657 SYBR® Green Supermix (BioRad, 172-5124) on a CFX Connect™ Real-Time System (BioRad)
658 with the BioRad CFX Manage 3.1 software. Each reaction was performed in duplicate and
659 relative mRNA quantities were normalized to the housekeeping gene RPL32. The B cell
660 Pou2f2 isoforms were amplified using the following primers : forward 5'
661 TGGTTCATTCCAGCATGGGG 3', reverse 5' TCCAGACTTTGCTTCTCGGC 3' and the spinal
662 Pou2f2 isoforms using : forward 5' CCACCATCACAGCCTACCAG 3', reverse 5'
663 GAGCTGGAGGAGTTGCTGTA 3' and RPL32 using: forward 5' GGCACCAGTCAGACCGATAT 3',
664 reverse 5' CAGGATCTGGCCCTTGAAC 3'. Relative expression changes between conditions
665 were calculated using the ΔΔCt method. All changes are shown as fold changes.
666

Acknowledgements

We thank members of the NEDI lab for material, technical support and discussions. We are grateful to Drs. T. Müller and H. Wende for kindly providing the guinea pig anti MafA and the rabbit anti cMaf antibodies, respectively, to Drs. F. Lemaigre and P. Jacquemin for the Hnf6/Oc2 double mutant mice, to Dr. C. Pierreux for the pCMV-MCS, to Dr. J. Ambroise for assistance with the microarray analyses and to Dr. L. Dumoutier for cDNAs of B lymphocytes. Work in the F.C. laboratory was supported by grants from the "Fonds spéciaux de recherche" (FSR) of the Université catholique de Louvain, by a "Projet de recherche (PDR)" #T.0117.13 and an "Equipement (EQP)" funding #U.N027.14 of the Fonds de la Recherche Scientifique (F.R.S.-FNRS, Belgium), by the "Actions de Recherche Concertées (ARC)" #10/15-026 of the "Direction générale de l'Enseignement non obligatoire et de la Recherche scientifique – Direction de la Recherche scientifique – Communauté française de Belgique" and granted by the "Académie universitaire 'Louvain'" and by the Association Belge contre les Maladies neuro-Musculaires. L.M.C. acknowledges funding from the Australian Government (NHMRC IRIIS and research grants #637306 and #575500) and Victorian State Government Operational Infrastructure Support. S.D. and C.B. hold PhD grants from the Fonds pour la Recherche dans l'Industrie et l'Agriculture (F.R.S.-FNRS, Belgium), M.H.-F. was a Postdoctoral Researcher of the F.R.S.-FNRS, F.C. is a Senior Research Associate of the F.R.S.-FNRS.

Competing interests: the authors declare no competing interest

689 **References**

690 Ampatzis, K., J. Song, J. Ausborn, and A. El Manira. 2014. "Separate microcircuit modules of
691 distinct v2a interneurons and motoneurons control the speed of locomotion."
692 *Neuron* 83 (4):934-43. doi: 10.1016/j.neuron.2014.07.018.
693 Audouard, E., O. Schakman, A. Ginion, L. Bertrand, P. Gailly, and F. Clotman. 2013. "The
694 Onecut transcription factor HNF-6 contributes to proper reorganization of Purkinje
695 cells during postnatal cerebellum development." *Mol Cell Neurosci* 56:159-68. doi:
696 10.1016/j.mcn.2013.05.001.
697 Audouard, E., O. Schakman, F. Rene, R. E. Huettl, A. B. Huber, J. P. Loeffler, P. Gailly, and F.
698 Clotman. 2012. "The Onecut transcription factor HNF-6 regulates in motor neurons
699 the formation of the neuromuscular junctions." *PLoS One* 7 (12):e50509. doi:
700 10.1371/journal.pone.0050509 PONE-D-12-19632 [pii].
701 Azim, E., J. Jiang, B. Alstermark, and T. M. Jessell. 2014. "Skilled reaching relies on a V2a
702 propriospinal internal copy circuit." *Nature* 508 (7496):357-63. doi:
703 10.1038/nature13021.
704 Barber, M., and A. Pierani. 2016. "Tangential migration of glutamatergic neurons and cortical
705 patterning during development: Lessons from Cajal-Retzius cells." *Dev Neurobiol* 76
706 (8):847-81. doi: 10.1002/dneu.22363.
707 Beaudry, J. B., C. E. Pierreux, G. P. Hayhurst, N. Plumb-Rudewiez, M. C. Weiss, G. G.
708 Rousseau, and F. P. Lemaigre. 2006. "Threshold levels of hepatocyte nuclear factor 6
709 (HNF-6) acting in synergy with HNF-4 and PGC-1alpha are required for time-specific
710 gene expression during liver development." *Mol Cell Biol* 26 (16):6037-46. doi:
711 26/16/6037 [pii] 10.1128/MCB.02445-05.
712 Beguin, S., V. Crepel, L. Aniksztejn, H. Becq, B. Pelosi, E. Pallesi-Pocachard, L. Bouamrane, M.
713 Pasqualetti, K. Kitamura, C. Cardoso, and A. Represa. 2013. "An epilepsy-related ARX
714 polyalanine expansion modifies glutamatergic neurons excitability and morphology
715 without affecting GABAergic neurons development." *Cereb Cortex* 23 (6):1484-94.
716 doi: 10.1093/cercor/bhs138.
717 Bikoff, J. B., M. I. Gabitto, A. F. Rivard, E. Drobac, T. A. Machado, A. Miri, S. Brenner-Morton,
718 E. Famojure, C. Diaz, F. J. Alvarez, G. Z. Mentis, and T. M. Jessell. 2016. "Spinal
719 Inhibitory Interneuron Diversity Delineates Variant Motor Microcircuits." *Cell* 165
720 (1):207-19. doi: 10.1016/j.cell.2016.01.027.
721 Blacklaws, J., D. Deska-Gauthier, C. T. Jones, Y. L. Petracca, M. Liu, H. Zhang, J. P. Fawcett, J.
722 C. Glover, G. M. Lanuza, and Y. Zhang. 2015. "Sim1 is required for the migration and
723 axonal projections of V3 interneurons in the developing mouse spinal cord." *Dev*
724 *Neurobiol* 75 (9):1003-17. doi: 10.1002/dneu.22266.
725 Boije, H., and K. Kullander. 2018. "Origin and circuitry of spinal locomotor interneurons
726 generating different speeds." *Curr Opin Neurobiol* 53:16-21. doi:
727 10.1016/j.conb.2018.04.024.
728 Borowska, J., C. T. Jones, D. Deska-Gauthier, and Y. Zhang. 2015. "V3 interneuron
729 subpopulations in the mouse spinal cord undergo distinctive postnatal maturation
730 processes." *Neuroscience* 295:221-8. doi: 10.1016/j.neuroscience.2015.03.024.
731 Borowska, J., C. T. Jones, H. Zhang, J. Blacklaws, M. Goulding, and Y. Zhang. 2013.
732 "Functional subpopulations of V3 interneurons in the mature mouse spinal cord." *J*
733 *Neurosci* 33 (47):18553-65. doi: 10.1523/JNEUROSCI.2005-13.2013.

Britz, O., J. Zhang, K. S. Grossmann, J. Dyck, J. C. Kim, S. Dymecki, S. Gosgnach, and M. Goulding. 2015. "A genetically defined asymmetry underlies the inhibitory control of flexor-extensor locomotor movements." *Elife* 4. doi: 10.7554/eLife.04718.

Camos, S., C. Gubern, M. Sobrado, R. Rodriguez, V. G. Romera, M. A. Moro, I. Lizasoain, J. Serena, J. Mallolas, and M. Castellanos. 2014. "Oct-2 transcription factor binding activity and expression up-regulation in rat cerebral ischaemia is associated with a diminution of neuronal damage in vitro." *Neuromolecular Med* 16 (2):332-49. doi: 10.1007/s12017-013-8279-1.

Catela, C., M. M. Shin, and J. S. Dasen. 2015. "Assembly and function of spinal circuits for motor control." *Annu Rev Cell Dev Biol* 31:669-98. doi: 10.1146/annurev-cellbio-100814-125155.

Clotman, F., P. Jacquemin, N. Plumb-Rudewiez, C. E. Pierreux, P. Van der Smissen, H. C. Dietz, P. J. Courtoy, G. G. Rousseau, and F. P. Lemaigre. 2005. "Control of liver cell fate decision by a gradient of TGF beta signaling modulated by Onecut transcription factors." *Genes Dev* 19 (16):1849-54. doi: 10.1101/gad.340305.

Clovis, Y. M., S. Y. Seo, J. S. Kwon, J. C. Rhee, S. Yeo, J. W. Lee, S. Lee, and S. K. Lee. 2016. "Chx10 Consolidates V2a Interneuron Identity through Two Distinct Gene Repression Modes." *Cell Rep* 16 (6):1642-52. doi: 10.1016/j.celrep.2016.06.100.

Corcoran, L. M., M. Karvelas, G. J. Nossal, Z. S. Ye, T. Jacks, and D. Baltimore. 1993. "Oct-2, although not required for early B-cell development, is critical for later B-cell maturation and for postnatal survival." *Genes Dev* 7 (4):570-82.

Corcoran, L. M., F. Koentgen, W. Dietrich, M. Veale, and P. O. Humbert. 2004. "All known in vivo functions of the Oct-2 transcription factor require the C-terminal protein domain." *J Immunol* 172 (5):2962-9.

Crone, S. A., K. A. Quinlan, L. Zagoraiou, S. Droho, C. E. Restrepo, L. Lundfald, T. Endo, J. Setlak, T. M. Jessell, O. Kiehn, and K. Sharma. 2008. "Genetic ablation of V2a ipsilateral interneurons disrupts left-right locomotor coordination in mammalian spinal cord." *Neuron* 60 (1):70-83. doi: S0896-6273(08)00677-6 [pii] 10.1016/j.neuron.2008.08.009.

Dasen, J. S. 2017. "Master or servant? emerging roles for motor neuron subtypes in the construction and evolution of locomotor circuits." *Curr Opin Neurobiol* 42:25-32. doi: 10.1016/j.conb.2016.11.005.

Del Barrio, M. G., R. Taveira-Marques, Y. Muroyama, D. I. Yuk, S. Li, M. Wines-Samuelson, J. Shen, H. K. Smith, M. Xiang, D. Rowitch, and W. D. Richardson. 2007. "A regulatory network involving Foxn4, Mash1 and delta-like 4/Notch1 generates V2a and V2b spinal interneurons from a common progenitor pool." *Development* 134 (19):3427-36. doi: dev.005868 [pii] 10.1242/dev.005868.

Dougherty, K. J., and O. Kiehn. 2010. "Firing and cellular properties of V2a interneurons in the rodent spinal cord." *J Neurosci* 30 (1):24-37. doi: 10.1523/JNEUROSCI.4821-09.2010.

Dougherty, K. J., L. Zagoraiou, D. Satoh, I. Rozani, S. Doobar, S. Arber, T. M. Jessell, and O. Kiehn. 2013. "Locomotor rhythm generation linked to the output of spinal shox2 excitatory interneurons." *Neuron* 80 (4):920-33. doi: 10.1016/j.neuron.2013.08.015.

Espana, A., and F. Clotman. 2012a. "Onecut factors control development of the Locus Coeruleus and of the mesencephalic trigeminal nucleus." *Mol Cell Neurosci* 50 (1):93-102. doi: 10.1016/j.mcn.2012.04.002.

780 Espana, A., and F. Clotman. 2012b. "Onecut transcription factors are required for the second
781 phase of development of the A13 dopaminergic nucleus in the mouse." *J Comp*
782 *Neurol* 520 (7):1424-41. doi: 10.1002/cne.22803.
783 Francius, C., and F. Clotman. 2010. "Dynamic expression of the Onecut transcription factors
784 HNF-6, OC-2 and OC-3 during spinal motor neuron development." *Neuroscience* 165
785 (1):116-29. doi: 10.1016/j.neuroscience.2009.09.076.
786 Francius, C., and F. Clotman. 2014. "Generating spinal motor neuron diversity: a long quest
787 for neuronal identity." *Cell Mol Life Sci* 71 (5):813-29. doi: 10.1007/s00018-013-
788 1398-x.
789 Francius, C., A. Harris, V. Rucchin, T. J. Hendricks, F. J. Stam, M. Barber, D. Kurek, F. G.
790 Grosveld, A. Pierani, M. Goulding, and F. Clotman. 2013. "Identification of multiple
791 subsets of ventral interneurons and differential distribution along the rostrocaudal
792 axis of the developing spinal cord." *PLoS One* 8 (8):e70325. doi:
793 10.1371/journal.pone.0070325.
794 Francius, C., M. Hidalgo-Figueroa, S. Debrulle, B. Pelosi, V. Rucchin, K. Ronellenfitch, E.
795 Panayiotou, N. Makrides, K. Misra, A. Harris, H. Hassani, O. Schakman, C. Parras, M.
796 Xiang, S. Malas, R. L. Chow, and F. Clotman. 2016. "Vsx1 Transiently Defines an Early
797 Intermediate V2 Interneuron Precursor Compartment in the Mouse Developing
798 Spinal Cord." *Front Mol Neurosci* 9:145. doi: 10.3389/fnmol.2016.00145.
799 Goetz, C., C. Pivetta, and S. Arber. 2015. "Distinct limb and trunk premotor circuits establish
800 laterality in the spinal cord." *Neuron* 85 (1):131-144. doi:
801 10.1016/j.neuron.2014.11.024.
802 Gosgnach, S., J. B. Bikoff, K. J. Dougherty, A. El Manira, G. M. Lanuza, and Y. Zhang. 2017.
803 "Delineating the Diversity of Spinal Interneurons in Locomotor Circuits." *J Neurosci*
804 37 (45):10835-10841. doi: 10.1523/JNEUROSCI.1829-17.2017.
805 Grossmann, K. S., A. Giraudin, O. Britz, J. Zhang, and M. Goulding. 2010. "Genetic dissection
806 of rhythmic motor networks in mice." *Prog Brain Res* 187:19-37. doi: 10.1016/B978-
807 0-444-53613-6.00002-2.
808 Guo, J., and E. S. Anton. 2014. "Decision making during interneuron migration in the
809 developing cerebral cortex." *Trends Cell Biol* 24 (6):342-51. doi:
810 10.1016/j.tcb.2013.12.001.
811 Hatzopoulos, A. K., A. S. Stoykova, J. R. Erselius, M. Goulding, T. Neuman, and P. Gruss. 1990.
812 "Structure and expression of the mouse Oct2a and Oct2b, two differentially spliced
813 products of the same gene." *Development* 109 (2):349-62.
814 Hayashi, M., C. A. Hinckley, S. P. Driscoll, N. J. Moore, A. J. Levine, K. L. Hilde, K. Sharma, and
815 S. L. Pfaff. 2018. "Graded Arrays of Spinal and Supraspinal V2a Interneuron Subtypes
816 Underlie Forelimb and Hindlimb Motor Control." *Neuron* 97 (4):869-884 e5. doi:
817 10.1016/j.neuron.2018.01.023.
818 Hilde, K. L., A. J. Levine, C. A. Hinckley, M. Hayashi, J. M. Montgomery, M. Gullo, S. P. Driscoll,
819 R. Grosschedl, Y. Kohwi, T. Kohwi-Shigematsu, and S. L. Pfaff. 2016. "Satb2 Is
820 Required for the Development of a Spinal Exteroceptive Microcircuit that Modulates
821 Limb Position." *Neuron* 91 (4):763-776. doi: 10.1016/j.neuron.2016.07.014.
822 Hodson, D. J., A. L. Shaffer, W. Xiao, G. W. Wright, R. Schmitz, J. D. Phelan, Y. Yang, D. E.
823 Webster, L. Rui, H. Kohlhammer, M. Nakagawa, T. A. Waldmann, and L. M. Staudt.
824 2016. "Regulation of normal B-cell differentiation and malignant B-cell survival by
825 OCT2." *Proc Natl Acad Sci U S A* 113 (14):E2039-46. doi: 10.1073/pnas.1600557113.

826 Jacquemin, P., S. M. Durviaux, J. Jensen, C. Godfraind, G. Gradwohl, F. Guillemot, O. D.
827 Madsen, P. Carmeliet, M. Dewerchin, D. Collen, G. G. Rousseau, and F. P. Lemaigre.
828 2000. "Transcription factor hepatocyte nuclear factor 6 regulates pancreatic
829 endocrine cell differentiation and controls expression of the proendocrine gene
830 ngn3." *Mol Cell Biol* 20 (12):4445-54.
831 Jacquemin, P., V. J. Lannoy, G. G. Rousseau, and F. P. Lemaigre. 1999. "OC-2, a novel
832 mammalian member of the ONECUT class of homeodomain transcription factors
833 whose function in liver partially overlaps with that of hepatocyte nuclear factor-6." *J*
834 *Biol Chem* 274 (5):2665-71.
835 Jacquemin, P., F. P. Lemaigre, and G. G. Rousseau. 2003. "The Onecut transcription factor
836 HNF-6 (OC-1) is required for timely specification of the pancreas and acts upstream
837 of Pdx-1 in the specification cascade." *Dev Biol* 258 (1):105-16. doi:
838 S0012160603001155 [pii].
839 Jacquemin, P., C. E. Pierreux, S. Fierens, J. M. van Eyll, F. P. Lemaigre, and G. G. Rousseau.
840 2003. "Cloning and embryonic expression pattern of the mouse Onecut transcription
841 factor OC-2." *Gene Expr Patterns* 3 (5):639-44. doi: S1567133X03001108 [pii].
842 Joshi, K., S. Lee, B. Lee, J. W. Lee, and S. K. Lee. 2009. "LMO4 controls the balance between
843 excitatory and inhibitory spinal V2 interneurons." *Neuron* 61 (6):839-51. doi:
844 10.1016/j.neuron.2009.02.011.
845 Kabayiza, K. U., G. Masgutova, A. Harris, V. Rucchin, B. Jacob, and F. Clotman. 2017. "The
846 Onecut Transcription Factors Regulate Differentiation and Distribution of Dorsal
847 Interneurons during Spinal Cord Development." *Front Mol Neurosci* 10:157. doi:
848 10.3389/fnmol.2017.00157.
849 Konig, H., P. Pfisterer, L. M. Corcoran, and T. Wirth. 1995. "Identification of CD36 as the first
850 gene dependent on the B-cell differentiation factor Oct-2." *Genes Dev* 9 (13):1598-
851 607.
852 Lai, H. C., R. P. Seal, and J. E. Johnson. 2016. "Making sense out of spinal cord somatosensory
853 development." *Development* 143 (19):3434-3448. doi: 10.1242/dev.139592.
854 Landry, C., F. Clotman, T. Hioki, H. Oda, J. J. Picard, F. P. Lemaigre, and G. G. Rousseau. 1997.
855 "HNF-6 is expressed in endoderm derivatives and nervous system of the mouse
856 embryo and participates to the cross-regulatory network of liver-enriched
857 transcription factors." *Dev Biol* 192 (2):247-57. doi: 10.1006/dbio.1997.8757.
858 Lannoy, V. J., A. Rodolosse, C. E. Pierreux, G. G. Rousseau, and F. P. Lemaigre. 2000.
859 "Transcriptional stimulation by hepatocyte nuclear factor-6. Target-specific
860 recruitment of either CREB-binding protein (CBP) or p300/CBP-associated factor
861 (p/CAF)." *J Biol Chem* 275 (29):22098-103. doi: 10.1074/jbc.M000855200
862 M000855200 [pii].
863 Latchman, D. S. 1996. "The Oct-2 transcription factor." *Int J Biochem Cell Biol* 28 (10):1081-
864 3.
865 Lee, S., B. Lee, K. Joshi, S. L. Pfaff, J. W. Lee, and S. K. Lee. 2008. "A regulatory network to
866 segregate the identity of neuronal subtypes." *Dev Cell* 14 (6):877-89. doi: S1534-
867 5807(08)00132-9 [pii] 10.1016/j.devcel.2008.03.021.
868 Lemaigre, F. P., S. M. Durviaux, O. Truong, V. J. Lannoy, J. J. Hsuan, and G. G. Rousseau. 1996.
869 "Hepatocyte nuclear factor 6, a transcription factor that contains a novel type of
870 homeodomain and a single cut domain." *Proc Natl Acad Sci U S A* 93 (18):9460-4.
871 Lillycrop, K. A., and D. S. Latchman. 1992. "Alternative splicing of the Oct-2 transcription
872 factor RNA is differentially regulated in neuronal cells and B cells and results in

protein isoforms with opposite effects on the activity of octamer/TAATGARAT-containing promoters." *J Biol Chem* 267 (35):24960-5.

Liu, Y. Z., K. A. Lillycrop, and D. S. Latchman. 1995. "Regulated splicing of the Oct-2 transcription factor RNA in neuronal cells." *Neurosci Lett* 183 (1-2):8-12.

Lu, D. C., T. Niu, and W. A. Alaynick. 2015. "Molecular and cellular development of spinal cord locomotor circuitry." *Front Mol Neurosci* 8:25. doi: 10.3389/fnmol.2015.00025.

Misra, K., H. Luo, S. Li, M. Matise, and M. Xiang. 2014. "Asymmetric activation of Dll4-Notch signaling by Foxn4 and proneural factors activates BMP/TGFbeta signaling to specify V2b interneurons in the spinal cord." *Development* 141 (1):187-98. doi: 10.1242/dev.092536.

Panayi, H., E. Panayiotou, M. Orford, N. Genethliou, R. Mean, G. Lapathitis, S. Li, M. Xiang, N. Kessaris, W. D. Richardson, and S. Malas. 2010. "Sox1 is required for the specification of a novel p2-derived interneuron subtype in the mouse ventral spinal cord." *J Neurosci* 30 (37):12274-80. doi: 10.1523/JNEUROSCI.2402-10.2010.

Pelosi, B., S. Migliarini, G. Pacini, M. Pratelli, and M. Pasqualetti. 2014. "Generation of Pet1210-Cre transgenic mouse line reveals non-serotonergic expression domains of Pet1 both in CNS and periphery." *PLoS One* 9 (8):e104318. doi: 10.1371/journal.pone.0104318.

Peng, C. Y., H. Yajima, C. E. Burns, L. I. Zon, S. S. Sisodia, S. L. Pfaff, and K. Sharma. 2007. "Notch and MAML signaling drives Scl-dependent interneuron diversity in the spinal cord." *Neuron* 53 (6):813-27. doi: S0896-6273(07)00139-0 [pii] 10.1016/j.neuron.2007.02.019.

Pierreux, C. E., V. Vanhorenbeeck, P. Jacquemin, F. P. Lemaigre, and G. G. Rousseau. 2004. "The transcription factor hepatocyte nuclear factor-6/Onecut-1 controls the expression of its paralog Onecut-3 in developing mouse endoderm." *J Biol Chem* 279 (49):51298-304. doi: 10.1074/jbc.M409038200 M409038200 [pii].

Pivetta, C., M. S. Esposito, M. Sigrist, and S. Arber. 2014. "Motor-circuit communication matrix from spinal cord to brainstem neurons revealed by developmental origin." *Cell* 156 (3):537-48. doi: 10.1016/j.cell.2013.12.014.

Roy, A., C. Francius, D. L. Rousso, E. Seuntjens, J. Debruyn, G. Luxenhofer, A. B. Huber, D. Huylebroeck, B. G. Novitch, and F. Clotman. 2012. "Onecut transcription factors act upstream of Isl1 to regulate spinal motoneuron diversification." *Development* 139 (17):3109-19. doi: 10.1242/dev.078501.

Stam, F. J., T. J. Hendricks, J. Zhang, E. J. Geiman, C. Francius, P. A. Labosky, F. Clotman, and M. Goulding. 2012. "Renshaw cell interneuron specialization is controlled by a temporally restricted transcription factor program." *Development* 139 (1):179-90. doi: 10.1242/dev.071134.

Stoykova, A. S., S. Sterrer, J. R. Erselius, A. K. Hatzopoulos, and P. Gruss. 1992. "Mini-Oct and Oct-2c: two novel, functionally diverse murine Oct-2 gene products are differentially expressed in the CNS." *Neuron* 8 (3):541-58.

Surmeli, G., T. Akay, G. C. Ippolito, P. W. Tucker, and T. M. Jessell. 2011. "Patterns of spinal sensory-motor connectivity prescribed by a dorsoventral positional template." *Cell* 147 (3):653-65. doi: S0092-8674(11)01210-4 [pii] 10.1016/j.cell.2011.10.012.

Sweeney, L. B., J. B. Bikoff, M. I. Gabitto, S. Brenner-Morton, M. Baek, J. H. Yang, E. G. Tabak, J. S. Dasen, C. R. Kintner, and T. M. Jessell. 2018. "Origin and Segmental Diversity of Spinal Inhibitory Interneurons." *Neuron* 97 (2):341-355 e3. doi: 10.1016/j.neuron.2017.12.029.

Talpalar, A. E., J. Bouvier, L. Borgius, G. Fortin, A. Pierani, and O. Kiehn. 2013. "Dual-mode operation of neuronal networks involved in left-right alternation." *Nature* 500 (7460):85-8. doi: 10.1038/nature12286.

Thaler, J. P., S. K. Lee, L. W. Jurata, G. N. Gill, and S. L. Pfaff. 2002. "LIM factor Lhx3 contributes to the specification of motor neuron and interneuron identity through cell-type-specific protein-protein interactions." *Cell* 110 (2):237-49. doi: S0092867402008231 [pii].

Theodorou, E., G. Dalembert, C. Heffelfinger, E. White, S. Weissman, L. Corcoran, and M. Snyder. 2009. "A high throughput embryonic stem cell screen identifies Oct-2 as a bifunctional regulator of neuronal differentiation." *Genes Dev* 23 (5):575-88. doi: 10.1101/gad.1772509.

Tripodi, M., A. E. Stepien, and S. Arber. 2011. "Motor antagonism exposed by spatial segregation and timing of neurogenesis." *Nature* 479 (7371):61-6. doi: nature10538 [pii] 10.1038/nature10538.

Vanhorenbeeck, V., P. Jacquemin, F. P. Lemaigre, and G. G. Rousseau. 2002. "OC-3, a novel mammalian member of the ONECUT class of transcription factors." *Biochem Biophys Res Commun* 292 (4):848-54. doi: 10.1006/bbrc.2002.6760 S0006291X02967604 [pii].

Wirth, T., A. Priess, A. Annweiler, S. Zwilling, and B. Oeler. 1991. "Multiple Oct2 isoforms are generated by alternative splicing." *Nucleic Acids Res* 19 (1):43-51.

Ziskind-Conhaim, L., and S. Hochman. 2017. "Diversity of molecularly defined spinal interneurons engaged in mammalian locomotor pattern generation." *J Neurophysiol* 118 (6):2956-2974. doi: 10.1152/jn.00322.2017.

946 **Figure legends**

947

948 **Figure 1.** OC factors are present in multiple subsets of V2 interneurons. **(A-I")**
949 Immunolabelings for OC, the V2a generic marker Chx10 and markers of V2a subpopulations
950 (Francius et al. 2013) on transverse spinal cord sections (brachial or thoracic levels) of e12.5
951 wild-type mouse embryos. In each figure, the right ventral quadrant of the spinal cord is
952 shown. Only HNF-6 is detected in Shox2+ V2a cells (arrow in A-C''), whereas the 3 OC are
953 present in the MafA+ and in the cMaf+ V2a subsets (arrows in D-I"). **(J-L")** Immunolabelings
954 for OC, the V2b generic marker Gata3 and MafA. The 3 OC proteins are detected in MafA+
955 V2b interneurons (arrows). **(M-O")** Immunolabelings for OC and the V2c marker Sox1
956 demonstrate that OC factors are present in a majority of V2c interneurons (arrows). Sox1 in
957 the ventricular zone labels neural progenitors. Scale bar = 50 µm.

958

959 **Figure 2.** OC factors regulate the diversification of the V2 interneurons. Immunolabelings on
960 transverse spinal cord sections (brachial or thoracic levels) of control or *Hnf6*$^{-/-}$;*Oc2*$^{-/-}$ double-
961 mutant embryos. At e12.5 **(A-C)** and e14.5 **(D)**, the production of the V2a Chx10+
962 interneurons is not altered in the absence of OC factors. Similarly, the number of
963 Shox2+ V2a is affected neither at e12.5 **(E-G)** nor at e14.5 **(H)**. In contrast, quantitative
964 analysis of control or *Hnf6*$^{-/-}$;*Oc2*$^{-/-}$ littermates at e12.5 **(I-K)** and at e14.5 **(L)** shows reduction
965 in MafA+ V2a interneurons in double mutants as compared to control embryos. Similarly,
966 the number of cMaf+ V2a interneurons is significantly reduced at e12.5 (**M-O**) and e14.5 (**P**)
967 in the absence of OC factors. At e12.5 **(Q-S)** and e14.5 **(T)**, the production of the V2b
968 interneurons is not affected in *Hnf6*$^{-/-}$;*Oc2*$^{-/-}$ embryos. The generation of the MafA+ V2b
969 interneurons is also unchanged at e12.5 **(U-W)** or e14.5 **(X)**. At e12.5 **(Y-AA)**, the number of
970 V2c interneurons is dramatically reduced in the absence of OC factors (Sox1 in the
971 ventricular zone labels neural progenitors). However, this is no longer the case at e14.5 **(BB)**.
972 Mean values ± SEM. * p≤0.05 ; ** p≤0.01 ; *** p≤0.001. Scale bar = 50 µm.

973

974 **Figure 3.** OC factors regulate the distribution of V2a interneurons. Distribution of V2a
975 interneurons on transverse section of the spinal cord in control or *Hnf6*$^{-/-}$;*Oc2*$^{-/-}$ double-
976 mutant embryos at brachial, thoracic or lumbar level (only the right hemisection is shown).
977 Two-dimension distribution graphs (left) show integration of cell distribution from multiple

sections of multiple embryos of each genotype. One-dimension graphs (right) compare density distribution in control (blue) and in double-mutant embryos (red) on the dorso-ventral (upper) or the medio-lateral (lower) axis of the spinal cord (see Materials and methods for details). **(A-C)** At e12.5 in control embryos, V2a interneurons distribute in 2 connected clusters, a major central group and a minor medial group, at each level of the spinal cord. **(D-L)** In mutant embryos, the relative cell distribution between the 2 clusters seems altered, with relatively less central cells at brachial level and less medial cells at lumbar levels (n=3, p≤0.001). **(M-X)** Altered V2a distribution on the mediolateral axis is confirmed at e14.5. **(M-O, S-X)** In control embryos, the 2 V2a groups coalesce in a more evenly-distributed population that occupied ~70% of the medio-lateral axis. **(P-X)** In mutant embryos, V2a interneurons remain segregated into 2 distinct, although connected, clusters with a majority of cells in medial position (n=3, p≤0.001). **(Y-VV)** Similar observations are made for the Shox2+ V2a subpopulation. At e12.5 in control embryos **(Y-AA)**, Shox2+ V2a distribute in a minor medial and a major lateral cluster. **(BB-JJ)** In mutant embryos, these cells are slightly more ventral at brachial level and distribute more evenly between the two clusters at brachial and lumbar levels (n=3, p≤0.001). **(KK-VV)** At e14.5, Shox2+ V2a in the mutant were slightly more ventral and remained more medial than in control embryos (n=3, p≤0.001).

Figure 4. OC factors regulate the distribution of V2b interneurons. **(A-C)** At e12.5 in control embryos, V2b cells are distributed in a major central (brachial level) or lateral (thoracic and lumbar levels) cluster with minor subsets located more medially (arrows) or ventrally (arrowheads). **(D-L)** In OC mutant embryos at e12.5, the major population remains more compact, more centrally located and slightly more ventral. In addition, the ventral V2b subset is significantly depleted (asterisks; n=3, p≤0.001). **(M-X)** Consistently, at e14.5, V2b interneurons in the central cluster are more compact in the absence of OC factors, and a small contingent of V2b migrating towards the medio-dorsal spinal cord in control embryos (arrowheads) is missing in OC mutant littermates (asterisks; n=3, p≤0.001 at brachial level; p=0.080 and 0.112 at thoracic and lumbar levels, repsectively).

Figure 5. OC factors control expression of spinal cord-specific isoforms of *Pou2f2*. **(A)** The different Pou2f2 isoforms present in the B cells (B_Pou2f2) are characterized by invariant

exons (dark grey) and alternative exons 4, 5, 8, 14 or 16 (light grey). They contain a POU-specific domain (light green) encoded by exons 9 and 10 and a POU-type homeodomain (dark green) encoded by exons 11 and 12. The 4 spinal Pou2f2 isoforms (S_Pou2f2.1 to S_Pou2f2.4) (identified in the spinal cord) are characterized by a distinct exon 1 (E1X in light orange), an additional exon E5b (dark orange) and alternative exons E1b and 4 (medium orange and light grey, respectively). The presence of E1b disrupts the reading frame and imposes the use of the ATG located in E2a, whereas the absence of E1b leaves open the use of the ATG located in E1X. The regions corresponding to the generic or to the E5b *in situ* hybridization probes are indicated. **(B-E)** Quantification of spinal Pou2f2 or B-cell isoforms by RT-qPCR. **(B)** In control spinal cords, spinal Pou2f2 isoforms are >30-fold more abundant than B-cell isoforms. **(C)** B cell Pou2f2 isoforms barely trend to increase in the absence of OC factors. **(D)** In contrast, spinal Pou2f2 isoforms are 2.6-fold overexpressed in *Hnf6*$^{-/-}$;*Oc2*$^{-/-}$ spinal cords. **(E)** In double mutant spinal cords, spinal Pou2f2 isoforms are >60-fold more abundant than B-cell isoforms. **(F-I)** *In situ* hybridization labelings on transverse sections (brachial level) of control or *Hnf6*$^{-/-}$;*Oc2*$^{-/-}$ spinal cords at e11.5 with **(F-G)** a generic *Pou2f2* probe complementary to spinal and to B-cell isoforms **(A)** or **(H-I)** a spinal isoform-specific probe corresponding only to exon E5b **(A)**. **(F, H)** In control embryos, *Pou2f2* is strongly expressed in ventral and in dorsal interneuron populations, and more weakly in the ventral motor neuron area. **(G, I)** In OC mutant embryos, *Pou2f2* is upregulated in interneuron populations and its expression is expanded in ventral populations (arrowheads) and in the motor neurons (arrows). * p≤0.05 ; ** p≤0.01. Scale bars = 50 µm.

Figure 6. The Pou2f2+ V2a interneurons are mislocated in the absence of OC factors. **(A-F)** Immunolabelings and quantification of Pou2f2+ V2a interneurons in control or *Hnf6*$^{-/-}$;*Oc2*$^{-/-}$ mutant embryos. At e12.5 **(A-B)** and e14.5 **(C-D)**, Pou2f2 is detected in V2a Chx10^{+} interneurons, and the number of Pou2f2-containing Chx10+ cells trends to increase but is not significantly different in the absence of OC factors **(E-F)**. **(G-DD)** Distribution of Pou2f2+ V2a interneurons on transverse section of the spinal cord in control or *Hnf6*$^{-/-}$;*Oc2*$^{-/-}$ double-mutant embryos. One-dimension graphs (lower) show density distribution on the dorso-ventral (left) or the medio-lateral (right) axis of the spinal cord. **(G-R)** At e12.5, cells in the central clusters are slightly reduced at brachial and at thoracic levels in the absence of OC factors (n=3, p≤0.001). **(S-DD)** At e14.5, a vast majority of V2a containing Pou2f2 settle in a

more medial position in *Hnf6*$^{-/-}$;*Oc2*$^{-/-}$ spinal cords (n=3, p≤0.001). Mean values ± SEM. Scale bar = 50 µm.

Figure 7. The Pou2f2+ V2b interneurons are mislocated in the absence of OC factors. **(A-F)** Immunolabelings and quantification of Pou2f2+ V2b interneurons in control or *Hnf6*$^{-/-}$;*Oc2*$^{-/-}$ mutant embryos. At e12.5 **(A-B)** and e14.5 **(C-D)**, Pou2f2 is present in V2b Gata3+ interneurons, but the number of Pou2f2+ V2b cells was not significantly increased **(E-F)**. **(G-DD)** Distribution of Pou2f2+ V2b interneurons on transverse section of the spinal cord in control or *Hnf6*$^{-/-}$;*Oc2*$^{-/-}$ double-mutant embryos. One-dimension graphs (lower) show density distribution on the dorso-ventral (left) or the medio-lateral (right) axis of the spinal cord. **(G-R)** At e12.5, Pou2f2-containing V2b are more central and slightly more ventral in the absence of OC factors (n=3, p≤0.001). **(S-DD)** At e14.5, this subset of V2b interneurons is more clustered on the medio-lateral axis in *Hnf6*$^{-/-}$;*Oc2*$^{-/-}$ spinal cords (n=3, p≤0.001). Mean values ± SEM. Scale bar = 50 µm.

Figure 8. V2 interneuron distribution is altered after misexpression of *Pou2f2.* Overexpression of *Pou2f2* in chick embryonic spinal cord after electroporation at HH14-16 and immunolabelings 72 hours after electroporation. **(A-B, O-P)** At HH27-28, *Pou2f2* overexpression does not impact the number of V2a (Chx10+) **(K)**, Shox2+ V2a **(L)**, V2b **(M)** or V2d **(N)** interneurons. **(C-J, Q-T)** In contrast, it alters V2 distribution. **(C-J)** In control spinal cord, V2a and Shox2+ V2a interneurons are distributed in two closely connected clusters on the medio-lateral axis of the neuroepithelium. In electroporated spinal cord, lateral migration is increased and a majority of V2a and Shox2+ V2a interneurons are clustered in a single central group with ectopic lateral extensions (arrows; n=3, p≤0.001). **(Q-T)** In control spinal cord, V2b are distributed in two groups along the medio-lateral axis with a majority of cells in the lateral cluster. In electroporated spinal cord, lateral migration of the V2b interneurons is reduced and a majority of cells is located in the medial cluster (n=3, p≤0.001). Mean values ± SEM. Scale bar = 50 µm.

Figure 9. Pou2f2 regulate the distribution of V2a interneurons. **(A-G)** Immunolabelings and quantification of V2a, Shox2+ V2a and V2d interneurons in control or *Pou2f2*$^{-/-}$ mutant embryos. **(A-B, E)** At e12.5, the production of the Chx10+ V2a interneurons is not altered in

absence of Pou2f2. **(C-D, F-G)** Similarly, neither the number of Shox2+ V2a nor the number of V2d interneurons are affected in *Pou2f2*$^{-/-}$ mutants. **(H-EE)** Distribution of V2a and Shox2+ V2a interneurons on transverse section of the spinal cord in control or *Pou2f2*$^{-/-}$ mutant embryos. One-dimension graphs (lower) show density distribution on the dorso-ventral (left) or the medio-lateral (right) axis of the spinal cord. **(H-S)** V2a distribution is affected in *Pou2f2*$^{-/-}$ mutants. As compared to the two V2a clusters observed in control embryos, Chx10+ cells are relatively more abundant in the medial cluster in *Pou2f2*$^{-/-}$ mutant embryos (n=3, p≤0.001). **(T-EE)** Similarly, Shox2+ V2a remained more medial at brachial level, but migrated more laterally at lumbar level (n=3, p≤0.001). Mean values ± SEM. Scale bar = 50 µm.

Figure 10. Pou2f2 regulate the distribution of V2b interneurons. **(A-G)** Immunolabelings and quantification of V2b interneurons in control or *Pou2f2*$^{-/-}$ mutant embryos. At e12.5, the production of the Gata3+ V2b interneurons is not affected by the absence of Pou2f2. **(D-O)** Distribution of V2b interneurons on transverse section of the spinal cord in control or *Pou2f2*$^{-/-}$ mutant embryos. One-dimension graphs (lower) show density distribution on the dorso-ventral (left) or the medio-lateral (right) axis of the spinal cord. **(D-O)** The distribution of V2b cells is altered in *Pou2f2*$^{-/-}$ mutants, as V2b interneurons remained more medial at thoracic level but migrated more laterally at lumbar level (n=3, p≤0.001). Mean values ± SEM. Scale bar = 50 µm.

Supporting figure legends

Supplementary Figure S1. OC factors regulate the diversification of the V2 interneurons. **(A-H'')** Immunolabelings of the V2a generic marker Chx10 and markers of V2a subpopulations on transverse spinal cord sections (brachial or thoracic levels) control or *Hnf6*$^{-/-}$*;Oc2*$^{-/-}$ mutant embryos at e14.5. Quantifications are shown in Fig 1. V2a **(A-B),** Shox2+ V2a (arrows) and V2d interneurons (**C- D''**, arrowheads) are present in both control and double mutant embryos. **(E-E'')** MafA is present in a V2a supbopulation in control embryos (arrows), **(F-F'')** but is not detected in Chx10+ cells in the absence of OC factors. **(G-G'')** Similarly**,** cMaf is

present in a subpopulation of V2a interneurons in control embryos (arrows), **(H-H'')** which is not the case in *Hnf6*$^{-/-}$;*Oc2*$^{-/-}$ embryos. **(I-L'')** Immunolabelings of the V2b generic marker Gata3 and the marker of V2b subpopulation, MafA. V2b **(I-J'')** and MafA+ V2b (**K-L''**, arrows) interneurons are present in control and in *Hnf6*$^{-/-}$;*Oc2*$^{-/-}$ embryos. **(M-N)** The number of V2c interneurons is unchanged is similarly detected in *Hnf6*$^{-/-}$;*Oc2*$^{-/-}$ embryos as compared to control embryos (delineated cells). Sox1 in the ventricular zone labels neural progenitors. Scale bar = 50 µm.

Supplementary Figure S2. Pou2f2 RT-PCR experiments and sequence of the spinal Pou2f2 exon 1b and exon 5b. Composite assembly of electrophoresis images of RT-PCR amplification products for *Pou2f2* isoform sequences on embryonic spinal cord or B-cell RNA samples. Water was used as a negative control (Ctl-). **(A)** Amplifications from exon 1 (E1) to E6 on embryonic spinal cord RNA samples (asterisk) fail to amplify the RNA isoforms detected in B cell samples. In contrast, amplifications from E7 to E9, from E10 to E12 and from E13 to E17 show at least one similar amplicon in spinal cord samples and in B cell samples. **(B)** Amplification from E1 (other forward primer) to E7 also fails to amplify *Pou2f2* spinal cord isoforms. In contrast, amplifications from E2, 3, 4 and 5 to E7 produce systematically longer amplicons in spinal cord samples (arrowheads) as compared to B cell samples. The E6 to E7 amplification is similar in both samples. **(C)** Amplifications from E1X (present in the X6 sequence) to E3 do not produce amplicon in B-cell samples (asterisk). Amplifications from E1X to E3 or to E5b on spinal cord samples systematically produce 2 amplicons (arrowheads). Amplifications of the E5b exon sequence, from E3 to E5b and from E5b to E7 produce expected amplicons in spinal cord samples. **(D)** Comparison of exon 1b and exon 5b sequences in the predicted X6 sequence and the sequenced embryonic spinal cord *Pou2f2* isoforms. Sequences of E1X, E2a and E5b exons align (100% identity) with the predicted X6 sequence. Sequence of the additional alterative exon 1b is shown. SD = Size standard, E = Exon, SC = Embryonic spinal cord, B = B lymphocytes.

Supplementary Figure S3. The number of Pou2f2+Shox2+ V2a interneurons is normal in *Hnf6*$^{-/-}$;*Oc2*$^{-/-}$ mutant embryos. Immunolabelings on transverse spinal cord sections (brachial or thoracic levels) of control or *Hnf6*$^{-/-}$;*Oc2*$^{-/-}$ mutant embryos. At e12.5 **(A-C)** and at e14.5

(D-F), the number of V2a containing Shox2 and Pou2f2 is unchanged in the absence of OC factors. Mean values ± SEM. Scale bar = 50 µm.

Supplementary Figure S4. Efficacy of pCMV-eGFP and pCMV-Pou2f2 co-electroporation in the chicken embryonic spinal cord. **(A-C)** eGFP (green, **B**) and Pou2f2 (red, **C**) are present in a vast majority of cells along the dorso-ventral axis of the spinal cord. Scale bar = 50 µm.

Supplementary Figure S5. The number of MafA+ or cMaf+ V2a interneurons is normal in *Pou2f2*$^{-/-}$ mutant spinal cords. Immunolabelings on transverse spinal cord sections (brachial or thoracic levels) of control or *Pou2f2*$^{-/-}$ mutant embryos at e12.5. **(A-F)** Absence of Pou2f2 does not impact on the number of MafA+ **(A-C)** or cMaf+ V2a interneurons **(D-F)**. Mean values ± SEM. Scale bar = 50 µm.

Supplementary Figure S6. The number of MafA-positive V2b interneurons or of the V2c interneurons is normal in *Pou2f2*$^{-/-}$ mutant spinal cords. Immunolabelings on transverse spinal cord sections (brachial or thoracic levels) of control or *Pou2f2*$^{-/-}$ mutant embryos at e12.5. **(A-B, E)** The number of MafA+ V2b interneurons is not significantly altered in the absence of Pou2f2. **(C-D, F)** Similarly, the production of V2c interneurons is not affected in *Pou2f2* mutants. Mean values ± SEM. Scale bar = 50 µm.

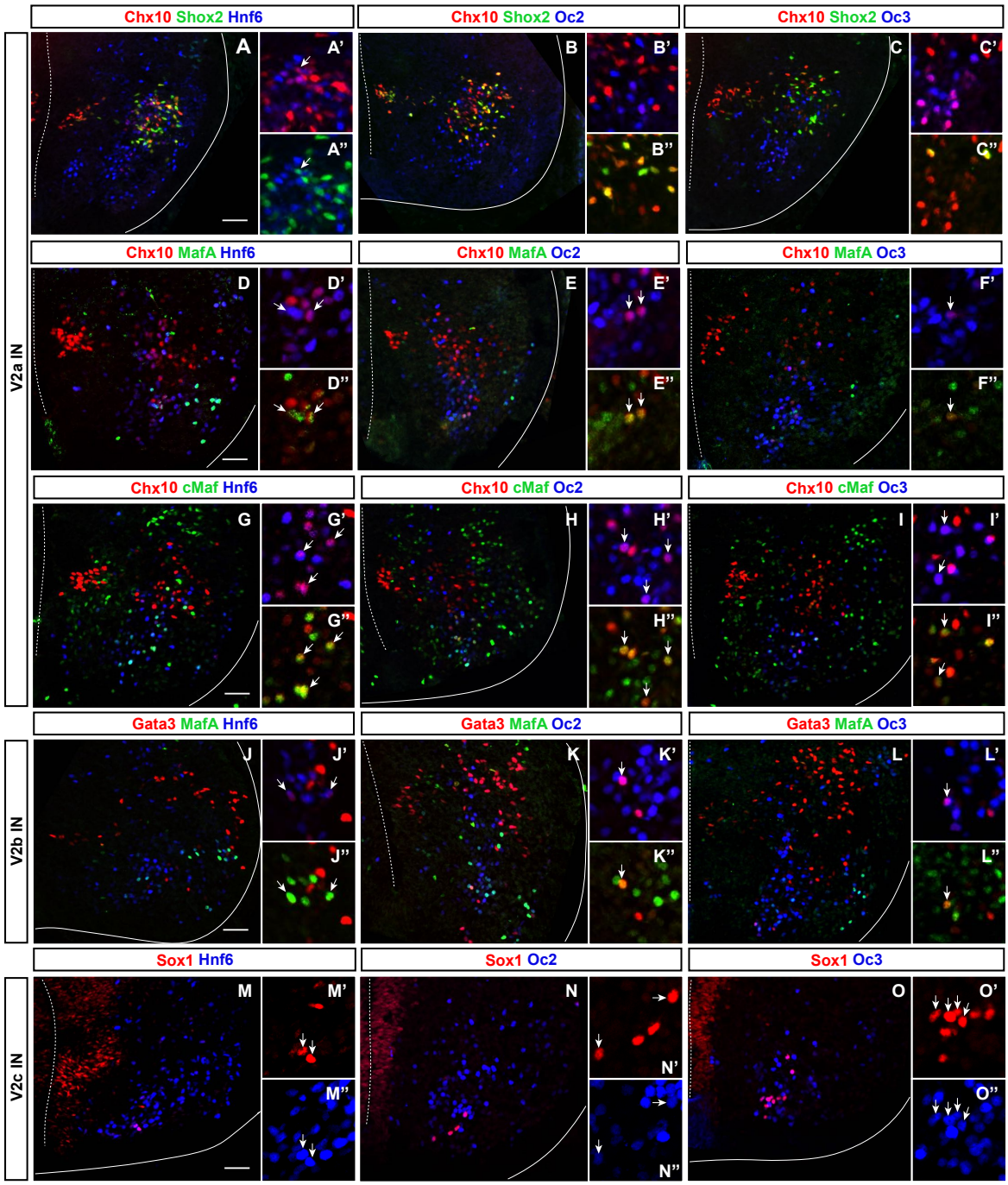

Harris A. et al, Figure 1

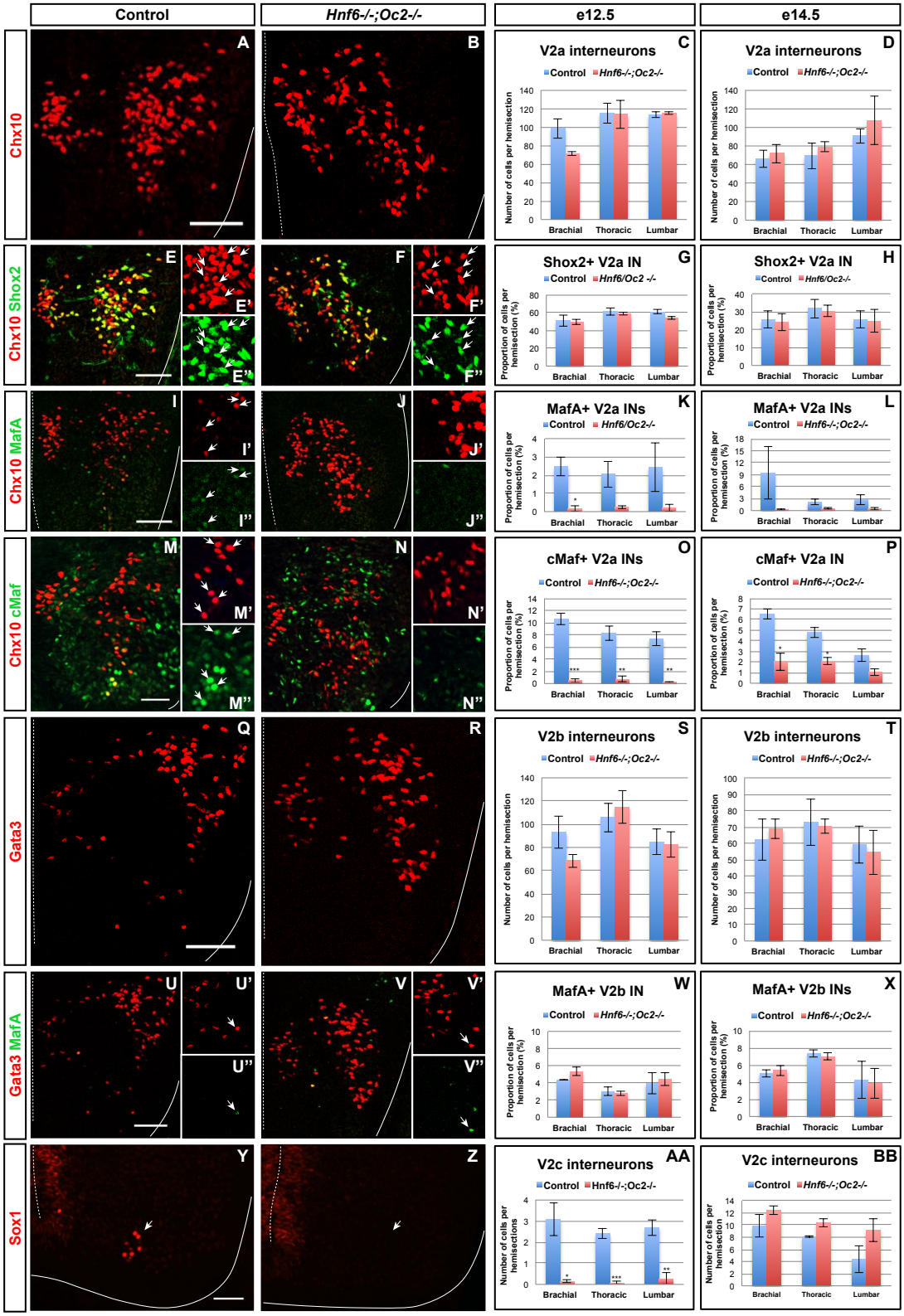

Harris A. et al., Figure 2

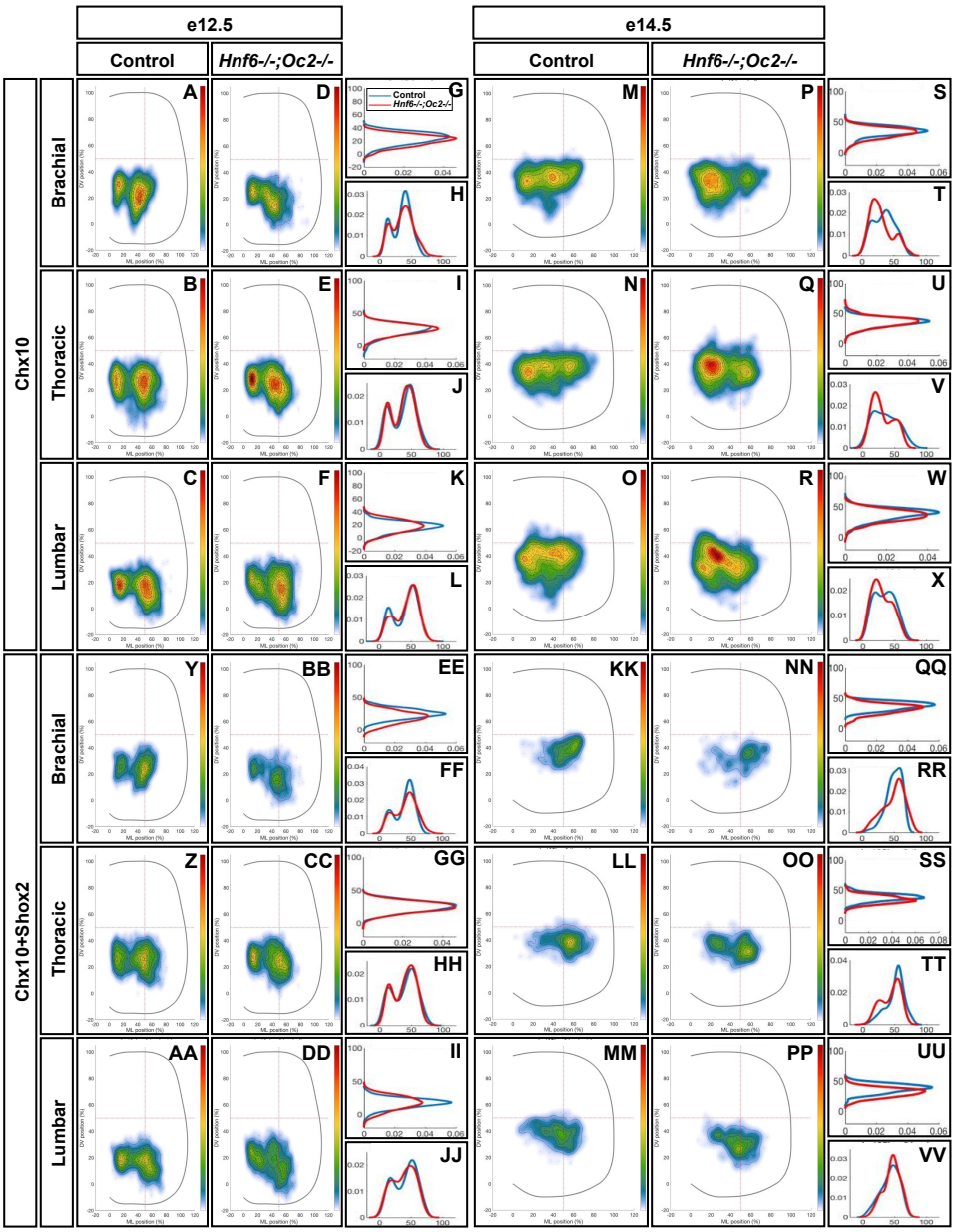

Harris A. et al, Figure 3

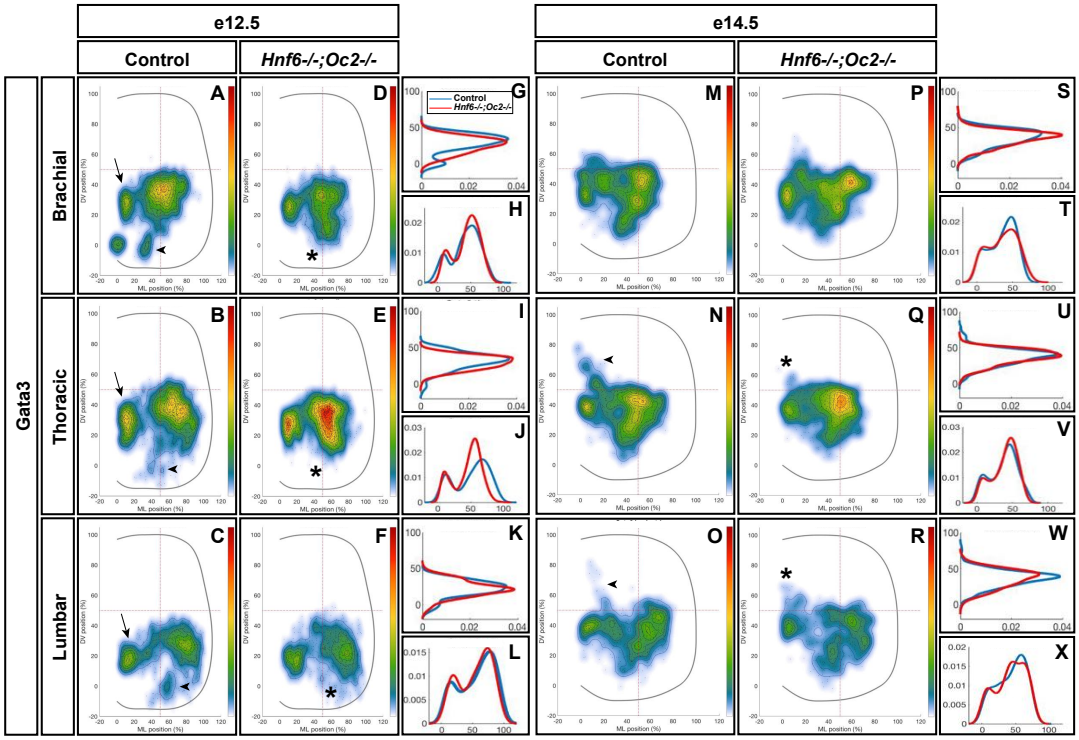

Harris A. et al, Figure 4

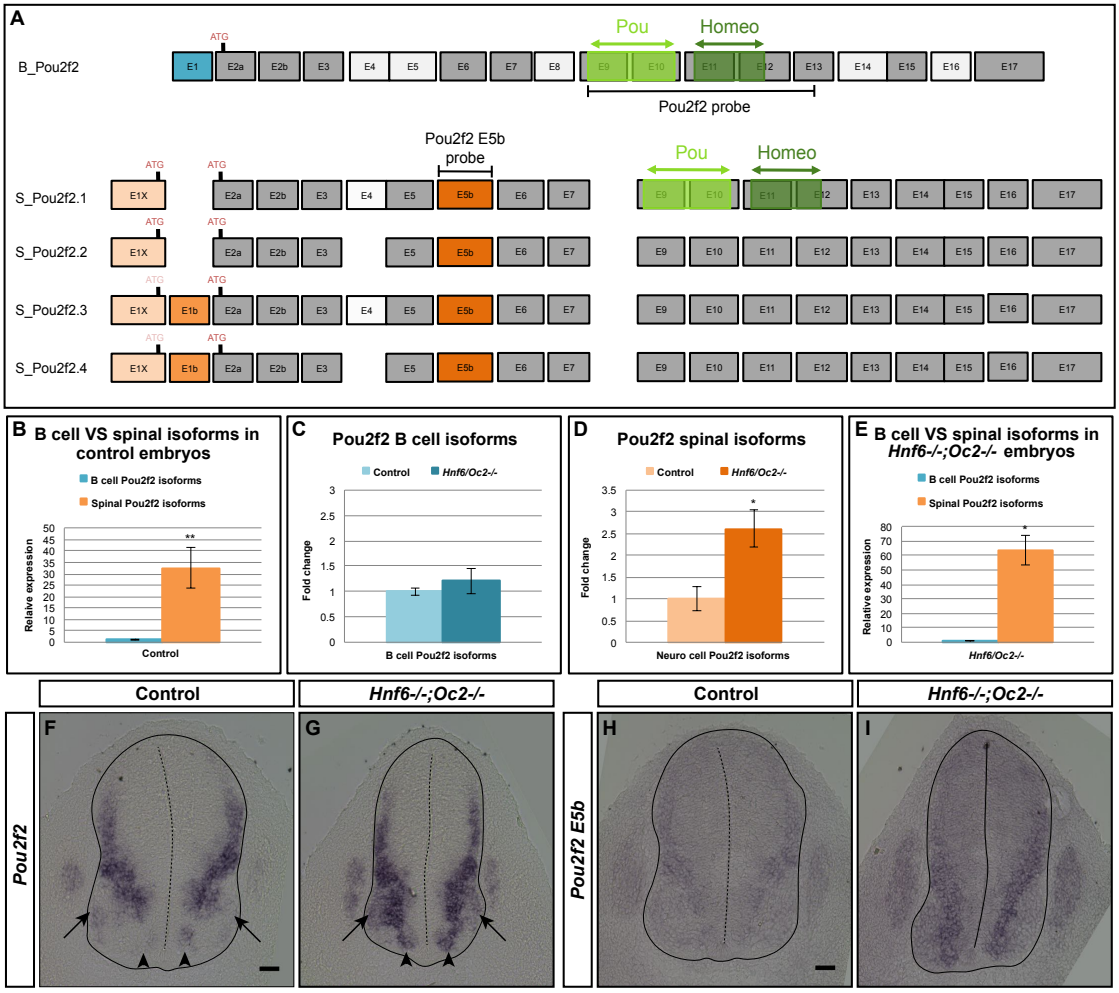

Harris A. et al, Figure 5

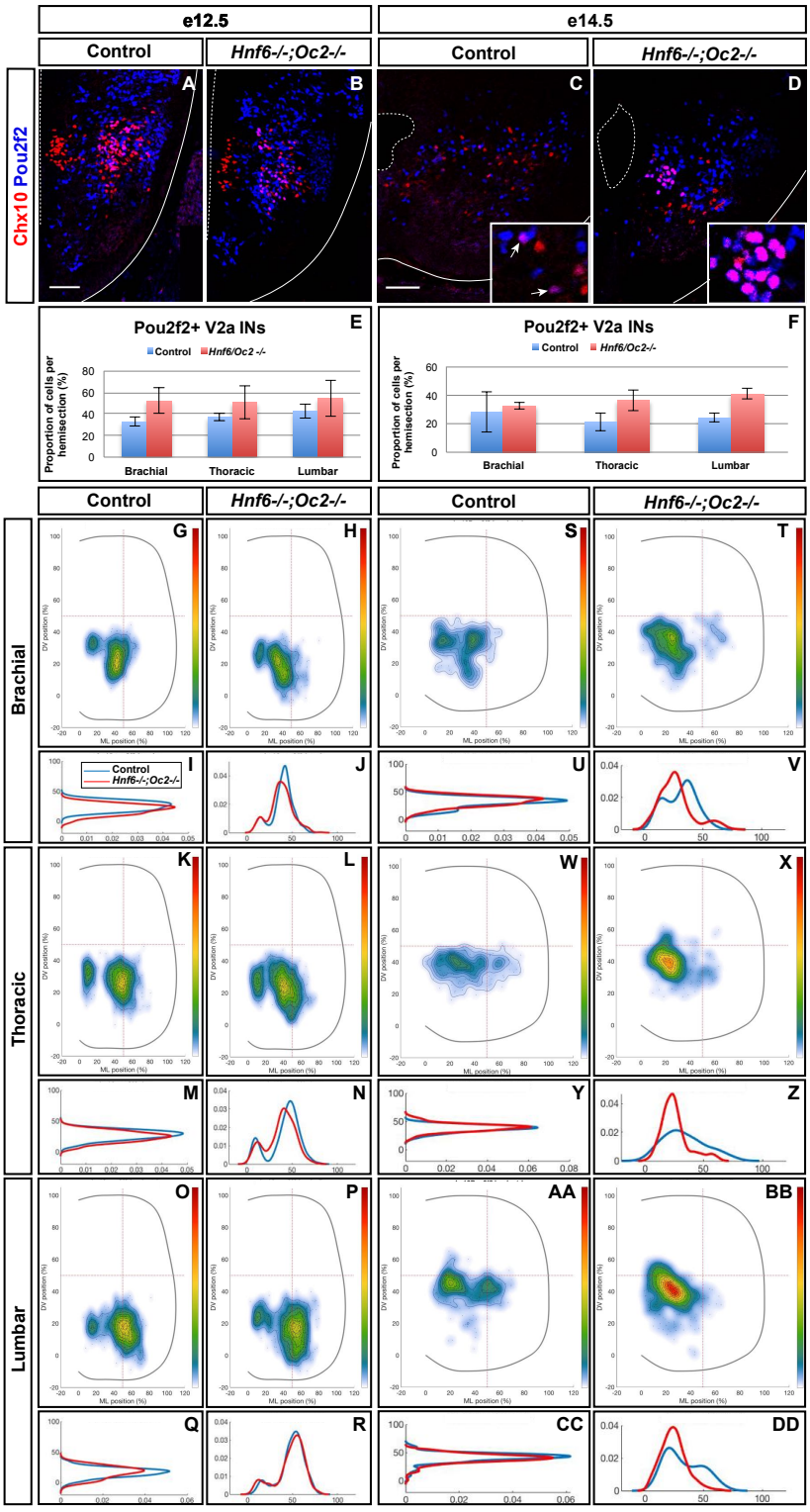

Harris A. et al, Figure 6

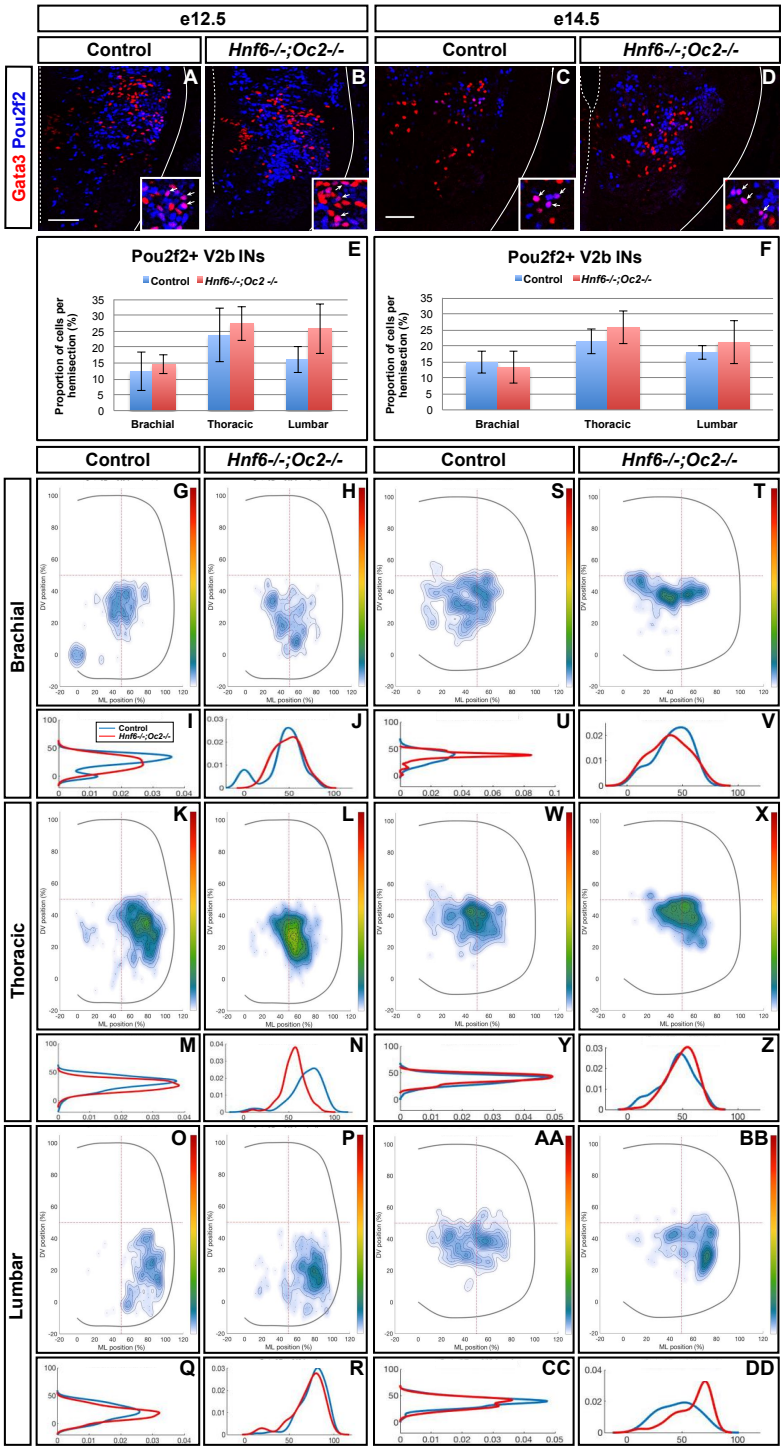

Harris A. et al, Figure 7

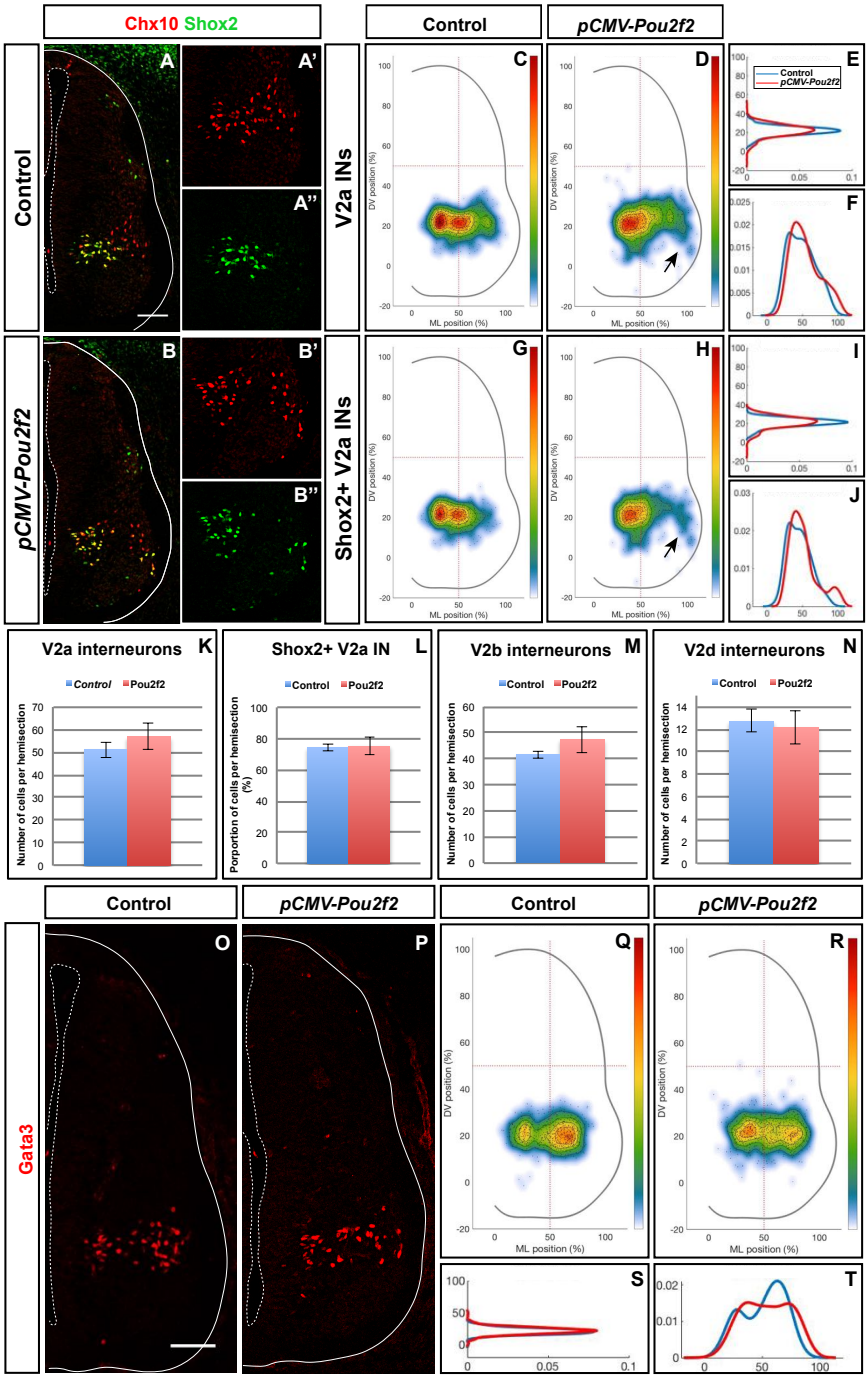

Harris A. et al., Figure 8

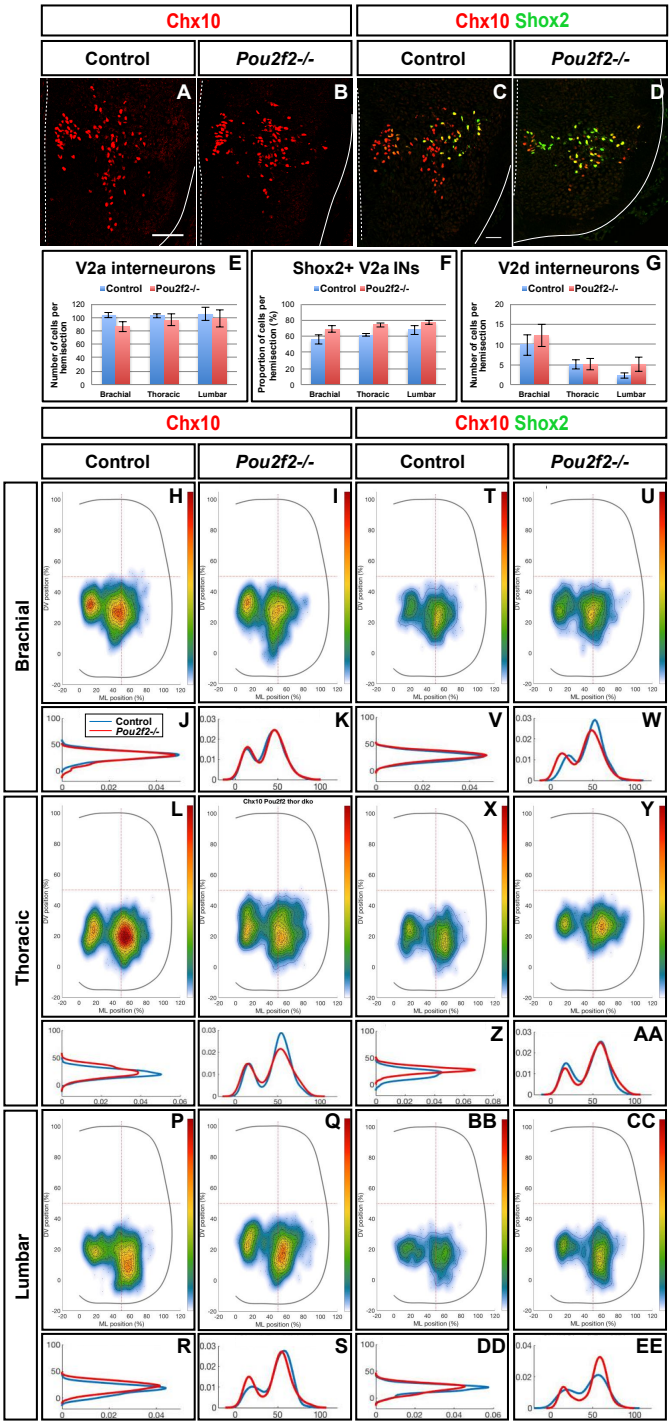

Harris A. et al, Figure 9

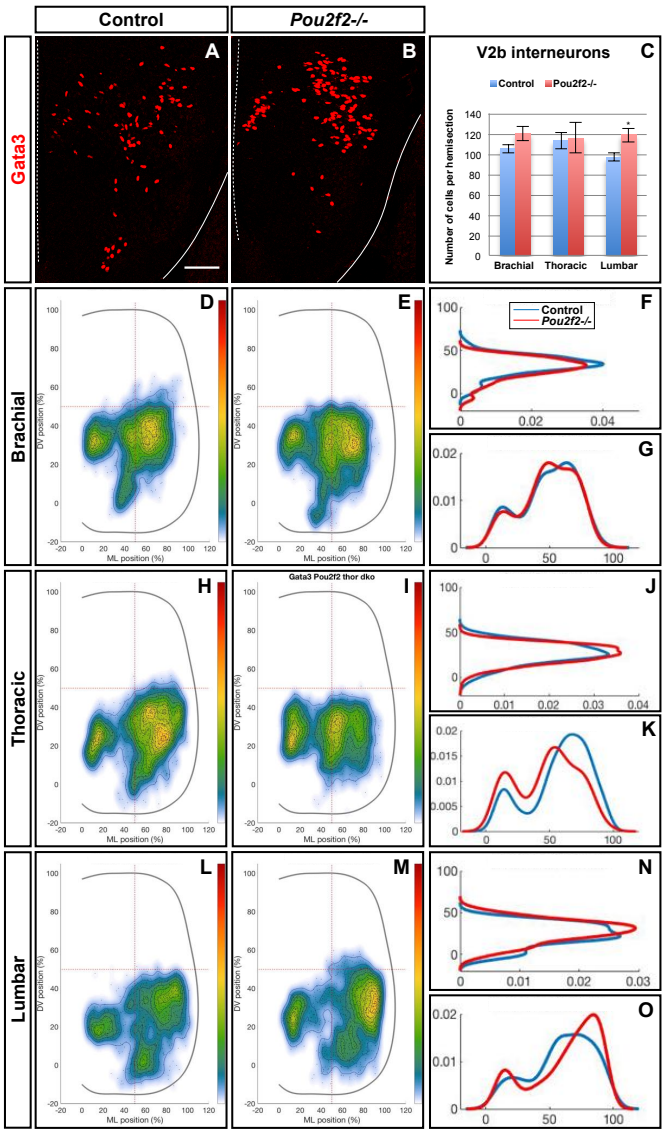

Harris A. et al, Figure 10

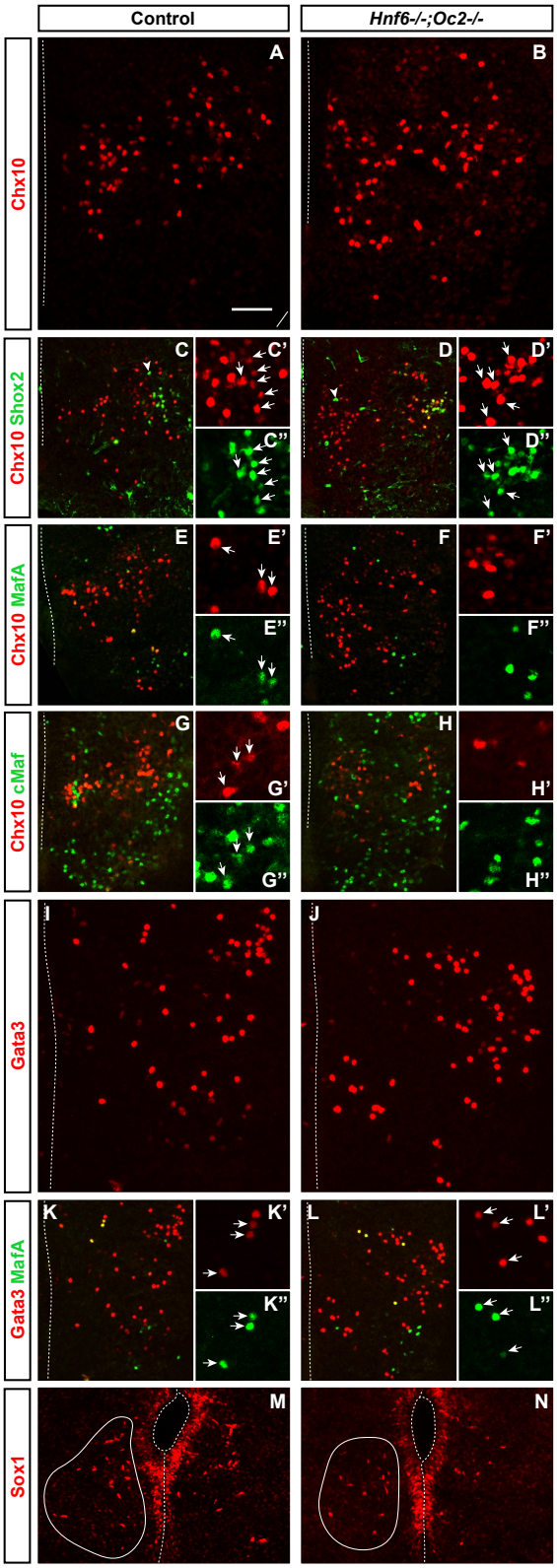

Harris A. et al., Supplementary figure 1

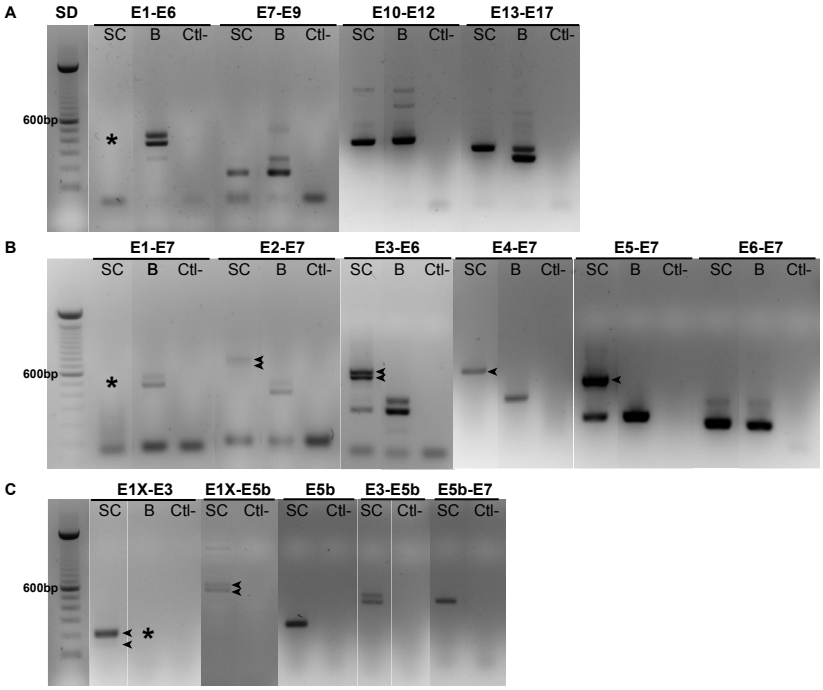

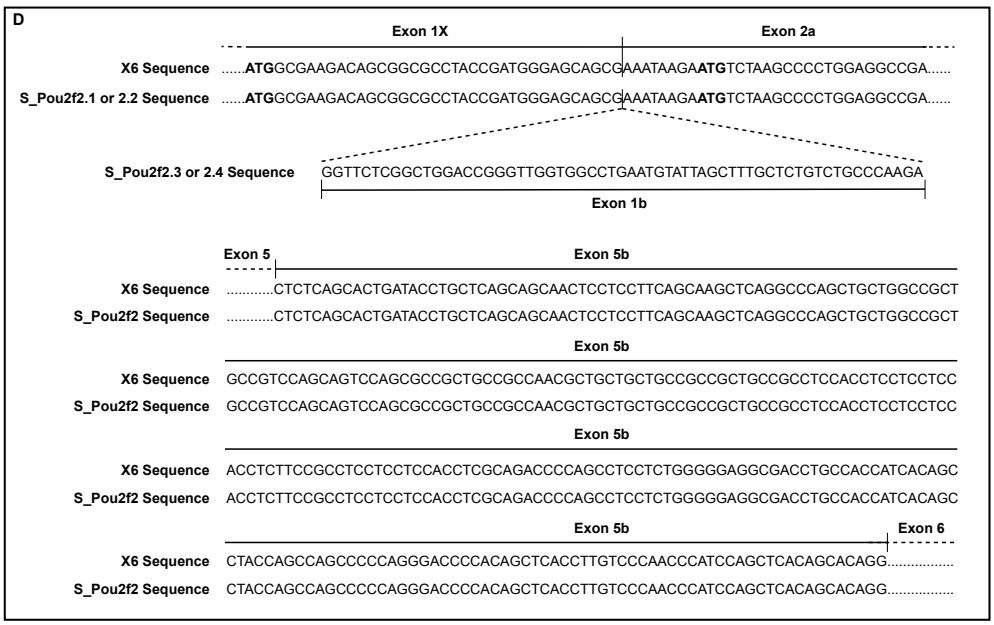

Harris et al., Supplementary figure 2

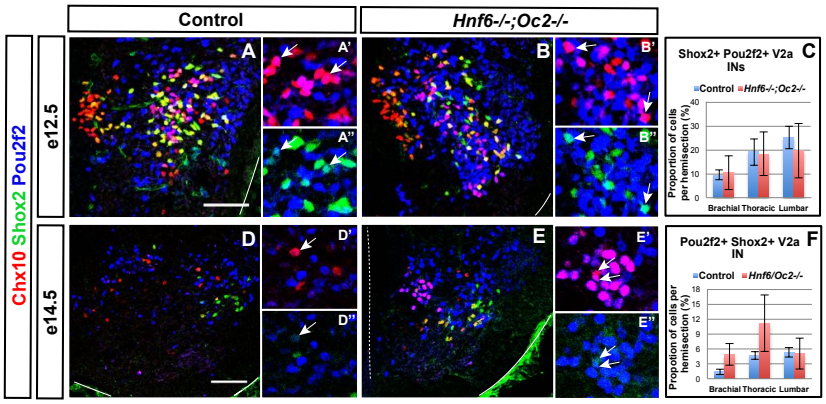

Harris A. et al, Supplementary figure 3

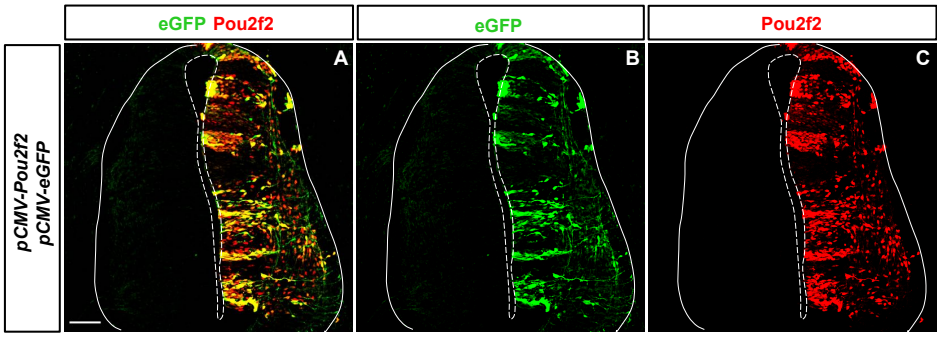

Harris A. et al, supplementary figure 4

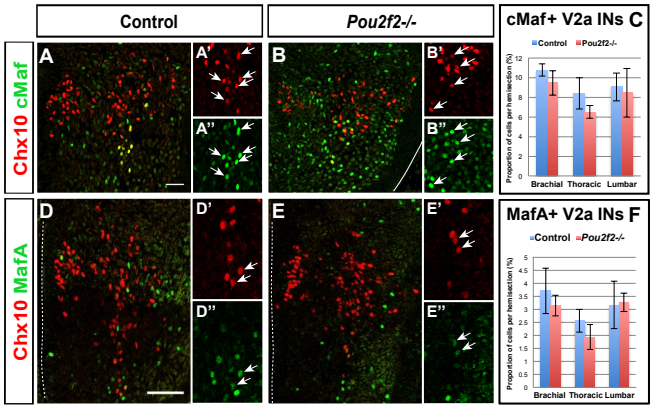

Harris A. et al, Supplementary figure 5

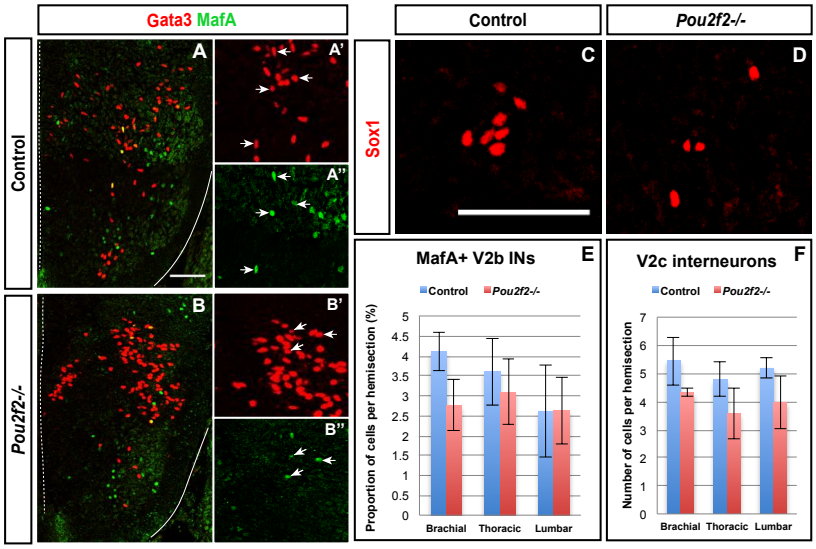

Harris A. et al., Supplementary figure 6